

DRAFT MANX following MICE at RAL DRAFT

Robert Abrams¹, Mohammad Alsharo²a¹, Charles Ankenbrandt¹, Emanuela Barzi²,
Kevin Beard¹, Alex Bogacz³, Daniel Broemmelsiek², Yu-Chiu Chao³,
Mary Anne Cummings¹, Yaroslav Derbenev³, Henry Frisch⁴, Ivan Gonin², Gail Hanson⁵,
David Hedin⁷, Martin Hu², Rolland Johnson¹, Stephen Kahn¹, Daniel Kaplan⁶,
Vladimir Kashikhin², Moyses Kuchnir¹, Michael Lamm², Valeri Lebedev²,
David Neuffer², Milord Popovic², Robert Rimmer³, Thomas Roberts¹, Richard Sah¹,
Linda Spentzouris⁶, Alvin Tollestrup², Daniele Turrioni², Victor Yarba²,
Katsuya Yonehara², Cary Yoshikawa², Alexander Zlobin²

¹*Muons, Inc.*

²*Fermi National Accelerator Laboratory*

³*Thomas Jefferson National Accelerator Facility*

⁴*University of Chicago*

⁵*University of California at Riverside*

⁶*Illinois Institute of Technology*

⁷*Northern Illinois University*

1 Executive Summary

The Muon Collider and Neutrino Factory Ionization Cooling Experiment (MANX) is proposed to test the theory, an example useful for stopping muon beams, and simulations of the Helical Cooling Channel (HCC) by constructing a helical solenoid (HS) magnet and installing it at the Rutherford-Appleton Laboratory (RAL) as part of the international Muon Ionization Cooling Experiment (MICE).

Because of its potential importance to Fermilab for muon cooling applications, including muon colliders, neutrino factories, and stopping muon beams, it is proposed that MANX be organized as a joint Fermilab-RAL project, where Fermilab is responsible for the magnet and detector upgrades and RAL provides the MICE beam line, where much of the MICE apparatus can be reused.

MANX will test the HCC concept in its momentum-dependent incarnation, where a muon beam will lose about half of its energy in a continuous absorber, the HS field strength will scale with the muon momentum, and no RF energy replacement is required. This approach has advantages in that the experiment will be less expensive and more timely for not needing about 150 MeV of RF and in that there is a proposed upgrade to the mu2e experiment for the Project-X era that could use the same HS magnet.

The momentum-independent incarnation of the HCC, where RF is used to keep the momentum nearly constant, is not tested directly in this version of MANX. However, the theory of the HCC, the technology of the HS, and simulations that involve 150 MeV of absorber will be tested to give confidence that the effectiveness of new muon cooling techniques, especially for collider use, can be accurately predicted. MANX is an appropriate \$10M intermediate step toward a \$100M useful muon cooling channel.

1	Executive Summary	1
2	Introduction and Motivation	3
3	Helical Cooling Channel.....	7
3.1	Principle of a Helical Cooling Channel.....	7
3.1.1	Motion in a Helical Cooling Channel.....	7
3.1.2	Continuous, Homogeneous Absorber in a Dispersive Magnetic Field.....	9
3.1.3	Characterization of a Momentum-Dependent Cooling Channel	10
3.1.4	HCC Pre-Cooler Simulation Example.....	12
3.2	Emittance Reduction and Matching with the MANX HCC.....	14
3.2.1	Emittance Matching to the Helical Solenoid	15
4	Experimental Method.....	18
4.1	Definition of Baseline Configuration.....	18
4.1.1	Conceptual View of Experiment Components	19
4.2	Differences between MANX and MICE.....	20
4.2.1	Beam Composition and Rates at 350MeV/c.....	21
4.2.2	Improved Time-of-Flight Detectors.....	21
4.2.3	Detector planes inside the HCC.....	26
4.2.4	Improved Particle Identification	31
5	Requirements for Measurements	33
5.1	Statistical Precision Needs	33
5.2	Systematics and Ancillary Measurements.....	33
6	Beams	33
6.1	MICE Beam Line	33
6.2	Test Beams at Fermilab.....	34
7	Simulations of Baseline Beam/Detector Configuration.....	35
8	Components Currently Available and Needed	35
8.1	Helical Solenoid and Matching Sections	35
8.2	Existing MICE Configuration and Adaptations Needed for MANX.....	35
8.3	Software	36
9	Schedule, Resources Needed, and Cost.....	37
9.1	Boundary conditions	37
9.2	MICE Schedule	37
9.3	Completion of HCC and Matching Sections.....	38
9.4	Responsibilities of Participating Groups and Needs from Fermilab Divisions ..	39
9.5	Completion of Additional Components Needed for MANX	39
9.6	Timeline for Building, Testing, Installing and Running the Experiment.....	40
9.7	Cost Estimate.....	40
9.7.1	Scope of Estimate	40
9.7.2	Estimate Methodology and Basis.....	40
9.7.3	Contingencies.....	40
10	MANX and Other Muon Collider and Neutrino Factory R&D.....	40
10.1	Relationship to the Muon Accelerator R&D 5-Year Plan.....	40
10.2	Relationship to MICE.....	42

2 Introduction and Motivation

MANX is an experiment to test the theory [1], an implementation example [2], and numerical modeling [3] of a helical cooling channel (HCC), which has several potential applications for the capture, ionization cooling, and manipulation of large-emittance muon beams.

The HCC theory, inspired by the Siberian Snake [4], combines a solenoid field with helical dipole and helical quadrupole field components to provide a large acceptance channel with nearly homogeneous fields. The field uniformity in a long cooling channel is particularly advantageous because the very large emittances of muon beams generate large resonance driving terms that can interact with periodic magnetic variations.

Emittance exchange in a HCC, which is required to achieve 6-dimensional cooling, can be achieved using wedge absorbers and/or a continuous homogeneous absorber. MANX also tests this newer method, where dispersion-generated path length dependence on momentum provides the required correlation between momentum and energy loss.

There are two versions of the HCC that have applications to cooling of muon beams – 1) momentum dependent, where the magnet field strengths scale with diminishing muon momentum as energy is lost in an absorber and 2) momentum or z-independent, where energy lost in the absorber is almost constantly replenished by RF cavities so that the magnet strengths are constant.

MANX will test the HCC concept in its momentum-dependent version, where a muon beam will lose about half of its energy in a continuous absorber, the HS field strength will scale with the muon momentum, and no RF energy replacement is required. This approach has advantages in that the experiment will be less expensive and more timely for not needing about 150 MeV of RF and in that there is a proposed upgrade to the mu2e experiment for the Project-X era that could use the same HS magnet.

The momentum-independent version of the HCC, where RF is used to keep the momentum nearly constant, is not tested directly in this version of MANX. However, the theory of the HCC, the technology of the HS, and simulations that involve about 150 MeV of absorber will be tested to give confidence that the effectiveness of new muon cooling techniques, especially for collider use, can be accurately predicted.

Both versions have applications to muon colliders and neutrino factories. Momentum-dependent cooling channels like MANX can be used for a pre-cooler, as discussed later, in which the initial muon beam energy is higher than required for subsequent coolers. The emergent energy is reduced to a value that is low enough for the next stage. The most efficient method for the next stage and six orders of magnitude of 6d cooling is with a momentum independent channel with high pressure RF acting as the continuous energy absorber, energy replacer, and breakdown suppressor. However, if for some reason the

pressurized RF cavities do not work as hoped, a MANX-like approach is another possibility, where momentum-dependent HCC segments are alternated with linac sections. A momentum-dependent cooling channel can also be used as a final cooling section to take advantage of very high fields made available by the latest generation of superconductors [5]. A momentum dependent channel can also be used to increase the intensity of stopping muon beams and can be important for the mu2e experiment upgrade for the Project-X era at Fermilab. The MANX HS magnet is very similar to the one that has been used for simulations of this mu2e improvement concept [6].

The possibility to have MANX sited at RAL as part of the MICE program [7] is very attractive with potential improvements to each experiment. MANX can benefit by gaining a debugged beam line and detectors along with the expertise and experience of a talented and dedicated group of scientists. MICE should also gain by having more access to support from a larger part of the physics and accelerator communities who have an interest in muon beams for muon colliders and stopping muon beams.

The RAL infrastructure and MICE developments can expedite MANX in many ways. The use of single particle measurements and techniques based more on High Energy Physics experience than traditional accelerator experiments is one of many examples.

Some of the differences and their consequences between the two experiments are discussed in later sections of this proposal. For example, going from 4d to 6d cooling implies greater required precision on longitudinal momentum measurements. This is discussed later in the section on time of flight counters with improved resolution. The total momentum precision is also relevant because MANX does not use RF cavities to replenish lost energy and will rely on measurement of invariant emittance to characterize cooling. Another important difference is that MANX will have considerably more absorber than MICE and a correspondingly larger cooling signal, even though in its initial configuration it will use liquid helium as an absorber instead of hydrogen as used by MICE.

Several simulation efforts [8]**Error! Bookmark not defined.** have confirmed the utility of the HCC approach to six-dimensional cooling of the muon beams. These simulations have involved the use of pressurized RF cavities that continuously replace the energy lost in the ionization cooling process. The ultimate HCC will involve new technologies now under development, namely high-pressure RF cavities and high-temperature superconductor used to produce very high magnetic fields at low temperature. However, we believe that a strong case has already been made that the HCC will be an essential component of any future muon cooling effort and that an experimental demonstration of 6D cooling using a HCC with a continuous absorber is the next logical step.

The MANX experiment being proposed is to make a HCC without RF to measure the reduction of the 6D invariant beam phase space in a HCC filled with a continuous liquid helium absorber. Without RF cavities or the high-pressure hydrogen gas that would normally fill them, MANX is a simpler experiment that can be done relatively quickly and inexpensively. In parallel to the MANX program, we are supporting an effort to

incorporate RF cavities into HCC designs for cooling channels where the muon beam momentum is almost constant, and we have an active R&D program for high pressure gas-filled RF cavities. A summary of activities related to this proposal is included as Appendix A of this document

One plan is to build the HCC and new detectors at Fermilab and then transport them to Rutherford Appleton Laboratory in the UK, where they would be employed in the existing MICE beam as a later phase of the MICE experiment. By using the MICE beam line and spectrometer elements the cost and time to prepare the experiment will be reduced. We have already received technical support from Fermilab in developing the 4-coil model of the HS and we are seeking approval of this proposal to build a longer version at Fermilab for the MANX experiment.

A Letter of Intent was submitted to the Fermilab AAC in May, 2006 for a six-dimensional muon cooling experiment, and an Updated Letter of Intent was subsequently submitted in July, 2007. The development of the MANX concept has largely been funded through SBIR and STTR [9] awards by Muons, Inc. with Fermilab as a research partner. At present there is funding to complete another year of work on the MANX proposal. In addition, Muons, Inc. has received another \$650,000 for the next two years to study ways to upgrade the mu2e experiment to take advantage of a larger proton flux that the Project-X would enable. This program is based on the use of a HCC magnet that is effectively the same as the MANX magnet.

Working under the Phase I MANX STTR grant and the Phase II funding of another grant with the Fermilab Technical Division, a very novel and strikingly simple design for a momentum-dependent HCC magnet was invented, based on a helical solenoid (HS). A paper comparing the new design with the conventional approach to such a magnet was presented at the 2006 Applied Superconductivity Conference [10].

This new HS design based on displaced coils also works well for the original HCC concept, where RF imbedded in the HCC keeps the beam energy relatively constant. Engineering studies are now underway to investigate how to feed the RF wave guides through the HCC coils. Subsequent work on this novel magnet design and additional advances on the MANX matching magnets and the incorporation of RF cavities in the design was reported at PAC07 [11]. A scheme to match the optics of upstream and downstream spectrometers to the HCC optics was also developed and reported at PAC07 [12].

Significant progress has been made recently in the development of HCC schemes.

- The high-pressure RF cavity experiment had good results, showing no maximum gradient degradation even in a strong magnetic field [13]. Recent calculations and simulations indicate that dense muon beams in a gaseous hydrogen cooling channel may require techniques to remove the electrons produced by ionization. First tests of the use of electron absorbing dopants in hydrogen gas have been made.
- The MuCool Test Area (MTA) beam line that will allow radiation testing of the high-pressure RF cavity has been funded and is expected to be installed by the end of 2008 and operational in the first quarter of 2009.
- The design of a series of HCC segments has been improved to operate with less stringent requirements on the magnetic and RF fields
- A new use of a HCC (which is very similar to the MANX design itself) is being developed to enhance the stopping beam for a muon to electron conversion experiment [14].
- Another new use of a HCC involves superimposing two periods to develop a varying dispersion function that is appropriate for extreme cooling schemes like Parametric-resonance Ionization Cooling (PIC) and Reverse Emittance Exchange (REMEX) [15].

3 Helical Cooling Channel

3.1 Principle of a Helical Cooling Channel

3.1.1 Motion in a Helical Cooling Channel

The motion of particles in a helical cooling channel is illustrated in figure 1. In order to cool the 6D emittance of a beam, the longitudinal emittance must be transferred to transverse emittance where ionization cooling is effective. This emittance exchange is accomplished in the HCC by superimposing a transverse helical dipole magnet and a solenoid magnet to make possible longitudinal as well as transverse cooling. The helical dipole magnet creates an outward radial force due to the longitudinal momentum of the particle while the solenoid magnet creates an inward radial force due to the transverse momentum of the particle, or

$$\begin{aligned} F_{h-dipole} &\approx p_z \times B_{\perp}; & b &\equiv B_{\perp} \\ F_{solenoid} &\approx -p_{\perp} \times B_z; & B &\equiv B_z \end{aligned}, \quad (1)$$

where B is the field of the solenoid, the axis of which defines the z axis, and b is the field of the transverse helical dipole at the particle position. These Lorentz forces are the starting point for the derivations of the stability conditions for particle motion discussed in reference [1].

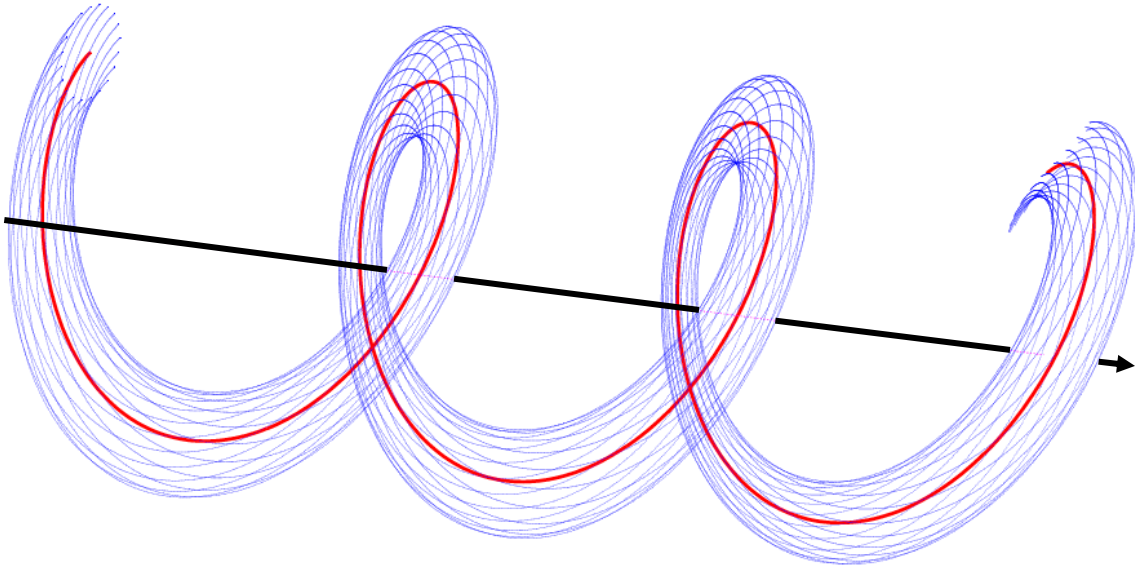


Figure 1 Illustration of motion of the beam about the z -axis (black), which coincides with the solenoid center. For a given momentum, muons (blue) oscillate about the periodic equilibrium orbit (red). This view in perspective shows 20 muons as they oscillate about the equilibrium orbit for three helix periods.

By moving to the rotating or helical frame of reference that moves with the field of the helical dipole magnet, a time and z -independent Hamiltonian is then developed to explore

the characteristics of particle motion in the magnetic fields of the channel. After this, a continuous homogeneous energy absorber is added. In continuous energy loss channels the strength of the solenoid field decreases along the length of the channel such that the radius of the equilibrium orbit remains constant. In energy replacement channels RF cavities compensate for the energy loss and thus maintain the radius of the equilibrium orbit. Equations describing six-dimensional cooling in this channel are also derived, including explicit expressions for cooling decrements and equilibrium emittances.

Some of the actual theoretical development of this cooling channel was worked out some years ago by Derbenev [16]. In that work, the absorber was seen as composed of a homogeneous part and a part with a density gradient. Since the thinking at the time was that the wedge absorber scheme shown in figure 2(a) should be dominant, especially in that discrete absorbers were always envisioned, the contributions from the homogeneous absorber were not considered as significant. The ideas and mathematical descriptions become more transparent in the case of a continuous homogeneous absorber. Much of the conceptual simplicity is lost in the case of discrete absorbers that must be carefully placed between magnetic coils and between RF cavities.

For a given beam momentum, one can vary the solenoid field and the strength and period of the helical dipole field. (The hydrogen gas energy-absorber density is also a free parameter provided the density is sufficient to suppress RF breakdown at the required level.) The helical field that must be superimposed on the solenoid field must have a quadrupole component in addition to the dipole component in order to give the beam additional stability. This component could be added with “ $\cos 2\theta$ ” quadrupole magnets having the same twist period as, and superimposed on, the helical dipole coils. Or, as we have learned in the last year, all three components can be provided by a helical solenoid magnet.

It is important to note that the direction of the solenoid field does not change in the cooling channel described below. This is an essential difference between the helical dipole method and the solenoid schemes with alternating field directions that have been envisioned up to now. This may also be some technical advantage to the extent that the large magnetic forces on the superconducting coils at the field reversal regions can be eliminated. Although a discussion of technical issues should follow the complete analysis of beam dynamics and cooling, we note that the use of continuous (or long) solenoids inherent in the helical concept should allow a higher maximum effective longitudinal field than that of schemes with alternating solenoid field directions. Consequently, the helical scheme will achieve a smaller equilibrium emittance, faster cooling rate, and decreased particle loss from decay.

A HCC incorporating hydrogen filled RF cavities will provide the fastest possible muon beam cooling because it will have the highest possible gradients due to the breakdown suppression of the dense gas in a magnetic field and because the same gas simultaneously acts as the energy absorber. However a HCC filled with liquid helium, without RF, is suitable for studying emittance exchange and reduction, and measurement of

transmission and losses in the HCC, particularly in the regions at the limits of the acceptance of the HCC.

Parametric-resonance Ionization Cooling and Reverse Emittance Exchange [17], new techniques for muon beams to get transverse emittances that are as small as those used in proton-antiproton colliders, are being investigated. In these schemes, a linear channel of dipoles and quadrupole or solenoid magnets periodically provides dispersion and strong focusing at the positions of beryllium wedge absorbers. Very careful compensation of chromatic and spherical aberrations and control of space charge tune spreads is required for these techniques to work. And most important with respect to the MANX experiment being proposed here, the initial emittances at the beginning of the periodic focusing channel must be small in all dimensions. Thus the HCC is the key to extreme muon beam cooling and to the Low Emittance Muon Collider [18].

3.1.2 Continuous, Homogeneous Absorber in a Dispersive Magnetic Field

Figure 2(a) is a conceptual picture of the usual mechanism for reducing the energy spread in a muon beam. The dispersion of the beam generated by the dipole magnet in figure 2(a) creates an energy-position correlation at a wedge-shaped absorber. Higher energy particles pass through thicker parts of the absorber and so have more energy loss than particles of less energy. After the absorber the beam becomes more mono-energetic.

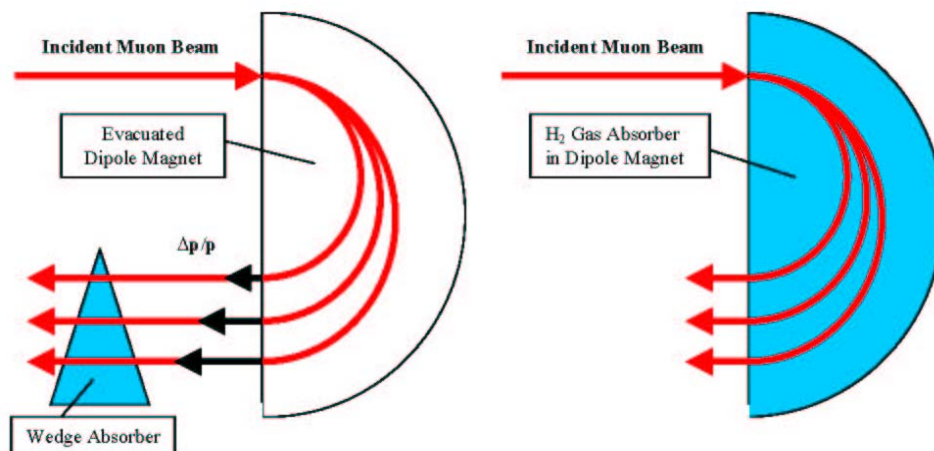


Figure 2 a) Wedge Absorber Technique b) Homogeneous Absorber Technique.

This process is called emittance exchange, because the transverse emittance must grow to allow the longitudinal emittance to be reduced. In Figure 1(a), the beam is in vacuum except in the wedge absorber. The process is limited by multiple scattering in the absorber and the high-Z windows that isolate the evacuated magnetic field region and the absorbers. For energy replacement type schemes, RF cavities, also in vacuum, replace the energy lost in the absorber.

In previous cooling plans, both the emittance exchange process and the transverse ionization beam cooling processes have been implemented by sequentially alternating absorbers and evacuated RF cavities.

The principle of emittance exchange by a continuous absorber in a dispersive magnetic field is shown in figure 2(b). In this case the energy loss depends on the dE/dx of the continuous absorber, where the longer path length of the higher momentum particles results in a greater energy loss than the shorter trajectories of the lower momentum particles. Thus the continuous absorber performs the same function as the wedge in figure 2(a). The same concept applies to pressurized RF cavities in which (hydrogen) gas filling the cavity acts both as the energy absorber for ionization cooling and as a breakdown suppressor to allow higher accelerating gradients.

3.1.3 Characterization of a Momentum-Dependent Cooling Channel

As discussed in the section above, the results of analytical calculations and numerical simulations of 6D cooling based on a HCC are very encouraging. In these studies, a long HCC encompasses a series of contiguous RF cavities that are filled with dense hydrogen gas so that the beam energy is kept nearly constant, where the RF continuously compensates for the energy lost in the absorber. In this case, the strengths of the magnetic solenoid, helical dipole, and quadrupole magnets of the HCC are also held constant. This feature of the HCC channel is exploited in the mathematical derivation of its properties, where the transverse field is subject only to a simple rotation about the solenoid axis as a function of distance, z , along the channel. This rotational invariance leads to a z - and time-independent Hamiltonian, which in turn allows the dynamical and cooling behavior of the channel to be examined in great detail. An important relationship between the momentum, p , for an equilibrium orbit at a given radius, a , and magnetic field parameters is derived in reference [Error! Bookmark not defined.], above:

$$p(a) = \frac{\sqrt{1 + \kappa^2}}{k} \left[B - \frac{1 + \kappa^2}{\kappa} b \right], \quad (2)$$

where B is the solenoid strength, b is the helical dipole strength at the particle position, k is the helix wave number ($k = 2\pi / \lambda$), and $\kappa \equiv ka = p_{\perp} / p_z$ is the tangent of the helix pitch angle.

Additional constraints to equation (2) are needed to determine the cooling properties of the channel. For example, to achieve equal cooling decrements in the two transverse coordinates and the longitudinal one:

$$q \equiv \frac{k_c}{k} - 1 = \beta \sqrt{\frac{1 + \kappa^2}{3 - \beta^2}} \quad (3)$$

Where $k_c = B\sqrt{1 + \kappa^2}/p$ is related to the cyclotron motion, q is an effective field index, and $\beta = v/c$. Another example, to achieve a condition where all the cooling is in the longitudinal direction, is to require that:

$$\hat{D} \equiv \frac{p}{a} \frac{da}{dp} = 2 \frac{1 + \kappa^2}{\kappa^2} \text{ and } q = 0.$$

Equation (2) is not just a description of the requirements for a simple HCC, but is also a recipe to manipulate field parameters to maintain stability for cases where one would like the momentum and/or radius of the equilibrium orbit to change for various purposes. Examples of variations on the original HCC concept that we have examined include:

- 1) A precooling device to cool a muon beam as it decelerates by energy loss in a continuous, homogeneous absorber, where the cooling can be all transverse, all longitudinal, or any combination. This device is discussed in the next section.
- 2) A device similar to a pre-cooler, but used as a full 6-dimensional muon cooling demonstration experiment (this MANX idea is the subject of this proposal).
- 3) A transition section between two HCC sections with different diameters. For example, this can be used when the RF frequency can be increased once the beam is sufficiently cold to allow smaller and more effective cavities and magnetic coils.
- 4) An alternative to the original HCC filled with pressurized RF cavities. In this alternate case, the muons would lose a few hundred MeV/c in a HCC section with momentum dependent fields and then pass through RF cavities to replenish the lost energy, where this sequence could be repeated several times.
- 5) A means to increase the rate of stopping muons for the mu2e experiment.
- 6) A pion decay/muon capture channel. The HCC can be looked at as comparable to a synchrotron in that it has an effective gamma-t such that a momentum compaction factor is one of its characteristics. Studies that have just begun are aimed at taking advantage of this to limit the time spread of the muons at the end of a decay channel to improve the capture rate for muons that can be eventually gathered into a single bunch for a muon collider.
- 7) A new invention is being developed as a channel for extreme muon cooling in which a HCC is used with two superimposed periodicities. By using two periods, the dispersion function can be made to change as a function of z such that the dispersion can be small at positions of the wedge absorbers needed for PIC or REMEX yet large where sextupole fields can be added for chromaticity correction.

3.1.4 HCC Pre-Cooler Simulation Example

Figure 3 shows the G4Beamline simulation of a combination vacuum decay section (40 m) and pre-cooler (5 m) HCC section. Pions and muons are created in the vacuum of the decay channel and captured in the HCC. At the end of the decay region, the muons pass through a thin aluminum window into a region of liquid energy absorber. By having a continuous HCC for the two sections, the problem of emittance matching into and out of the pre-cooler has been avoided. Simulation studies of various pre-cooler dimensions and magnet strengths have been done. Figure 4 shows an expanded view of the upstream end of the decay channel, and Figure 5 shows an expanded view of the pre-cooler. One can see that there are predominantly pions entering the decay channel and muons exiting the decay channel.

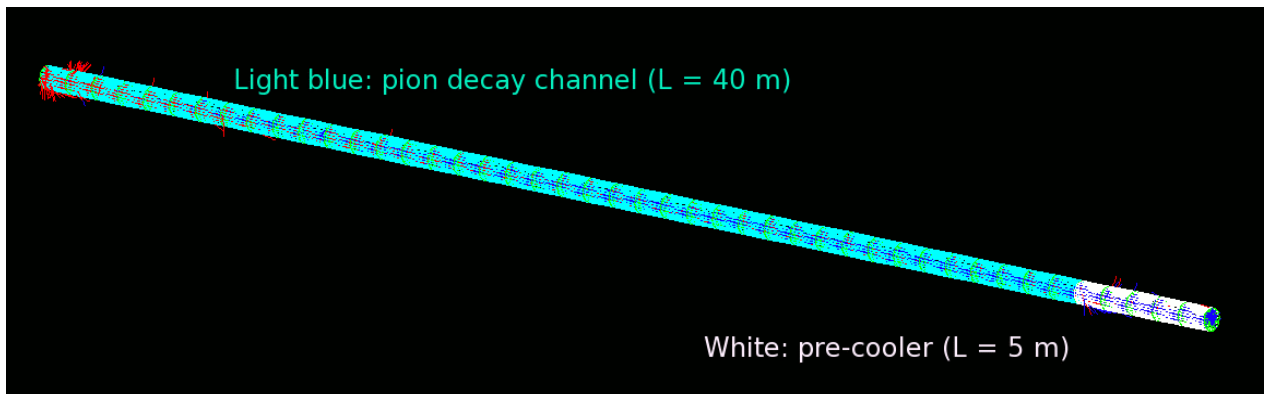


Figure 1 G4Beamline display of a 40 m pion decay channel (light blue) followed by a 5 m pre-cooling HCC (white). The red and blue lines show the pion and muon trajectories, respectively.

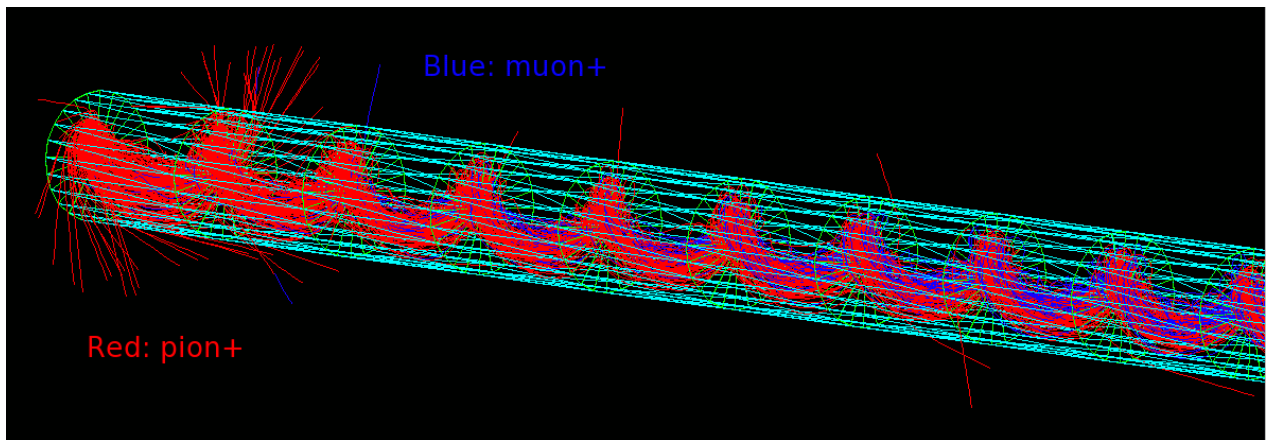


Figure 2 Detail of beginning of decay channel, pions are shown in red, muons in blue

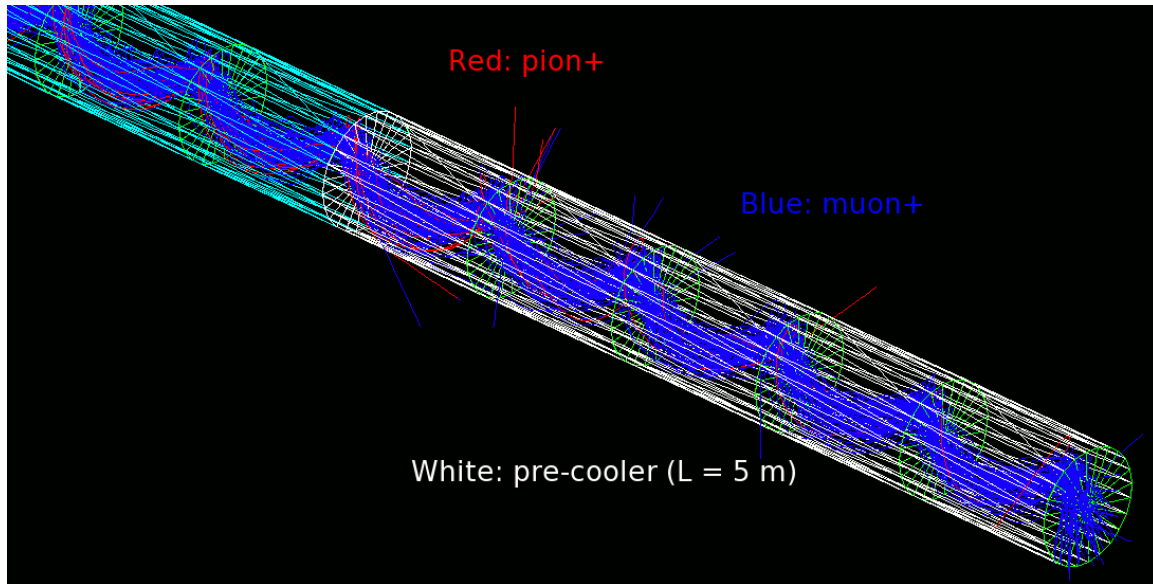


Figure 3 Details of trajectories in a pre-cooler. The helix period is 1 meter.

Figure 6 shows the normalized average emittance evolution of the beam in figure 5 as a function of the distance down the channel indicating the effect of liquid hydrogen and liquid helium and the effects of the aluminum containment windows of a 6 m long pre-cooler section. In this simulation, 400 MeV/c muons are degraded to less than 200 MeV/c in making 6 turns in a HCC filled with liquid hydrogen or liquid helium, without or with 1.6 mm aluminum windows on each end of the section. Far above the equilibrium emittances the cooling with liquid helium absorber is almost as good as with liquid hydrogen and the aluminum windows do not significantly degrade the cooling.

The settings of the helical dipole and quadrupole magnets and the solenoid are chosen to give equal cooling decrements in all three planes. The combined 6D cooling factor is 6.5 for liquid helium and 8.3 for liquid hydrogen. The improved performance of this HCC simulation relative to designs in which short flasks of liquid absorber alternate with RF cavities comes from the effectiveness of the HCC, from the greater path length in the absorber ($6 / \cos(45^\circ) = 8.5$ m), and from less heating by the high-Z windows. MICE, for example, has several aluminum windows for hydrogen containment and separation from RF cavities, while the two thin windows needed for this pre-cooler design are negligible in their heating effect compared to the length of the liquid absorber. This pre-cooling example inspired the idea of a 6D cooling demonstration experiment that is described below. In fact, the device that we propose to design as a 6D demonstration experiment also serves as a pre-cooler prototype.

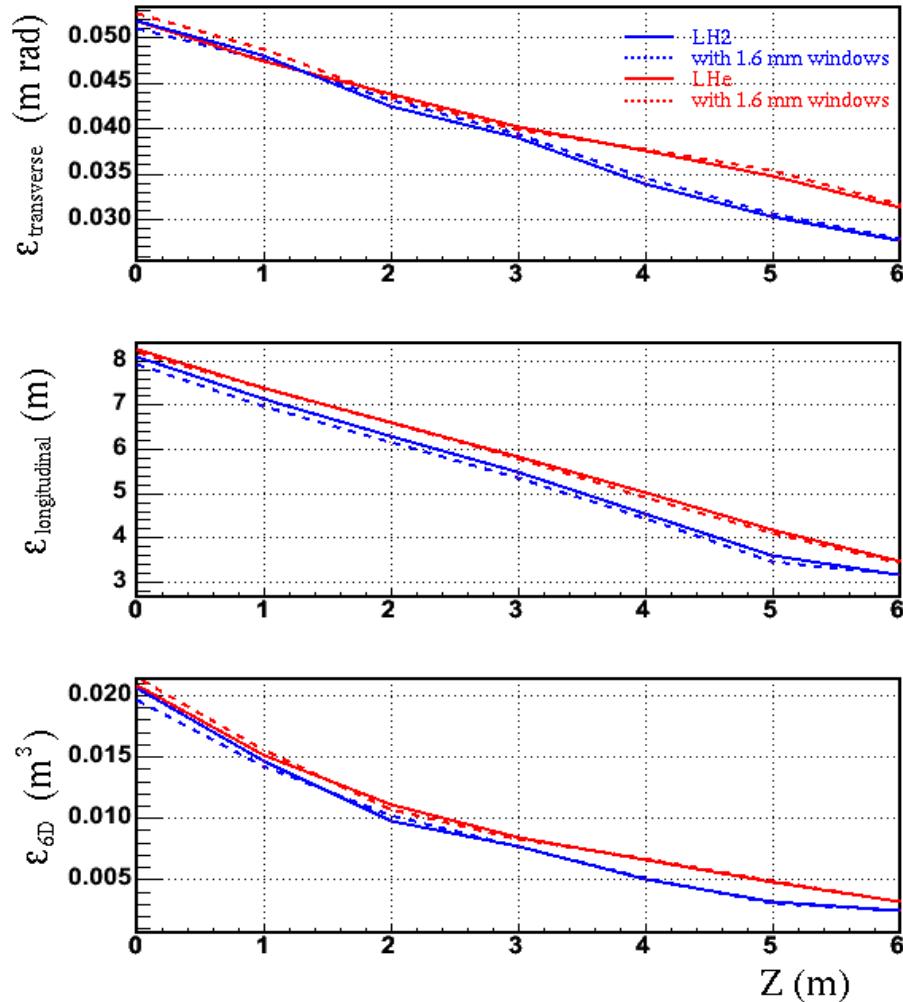


Figure 4 Simulations showing normalized emittance evolution for particles that survive to 6 m for a HCC pre-cooler filled with liquid hydrogen (blue) or liquid helium (red), with (dashed) and without (solid) 1.6 mm thick aluminum windows on each end.

The reduced cooling factors of MANX designs discussed later relative to this pre-cooling example reflect compromises in parameters such as initial momentum and length of the HCC and also less than perfect emittance matching.

3.2 Emittance Reduction and Matching with the MANX HCC

Typically, helical multipole fields that are used as Siberian Snake magnets for spin manipulation have fields that vary with the imaginary Bessel function $I_n(nkr)$. This function grows exponentially at moderately large radius. For the relatively modest field requirements on the HCC orbit, the field at the multipole coils would not be easily realized. A new magnetic coil arrangement, with only one quarter the field volume of the original HCC concept, has been invented, which is practical and designed to be readily built. This design can be applied to all HCC types, including MANX with its z-dependent field strengths. The simple scheme shown in Figure 7 is sufficient to create the three essential HCC magnetic field components: solenoid, helical dipole (as in the Siberian Snake), and helical quadrupole. (Although we have added a helical sextupole in some of

the simulations, the sextupole typically improves the acceptance by only 10% and is not needed for MANX.) The fields at the coils for this new arrangement are modestly higher than that seen at the reference orbit, making this helical solenoid feasible to implement.

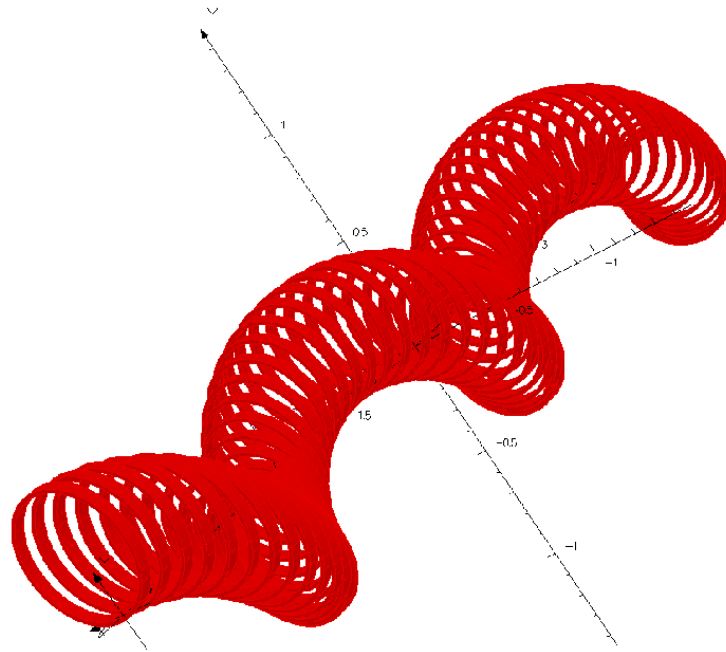


Figure 5 *Conceptual picture of a HCC segment using the helical solenoid, which provides solenoid, helical dipole, and helical quadrupole fields. Although at first glance it looks like a child’s “slinky” toy, the coils are independent rings. For the MANX simulation shown in the next figures below, each ring diameter is 0.5 m and ~60 coils are used for the 3.2 m long HCC.*

3.2.1 Emittance Matching to the Helical Solenoid

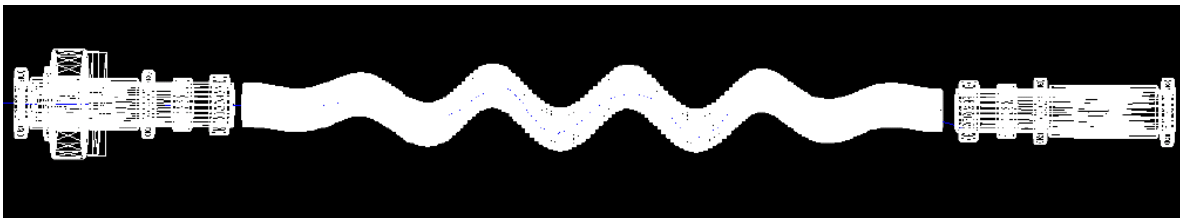


Figure 6 *G4beamline representation of MANX HCC with 1.5 period long matching sections positioned between the MICE spectrometers*

We are studying the matching of the MANX HCC to the existing MICE spectrometers. The most effective scheme to match the optics of the MANX HCC to MICE spectrometers is shown in Figure 8. This figure shows a 1.5 period long matching section before and after the 2 period long HCC. In the matching region, the coil radial position is varied linearly from solenoid axis to the start of the HCC keeping the same helix wave number. Similarly the helical dipole field is varied linearly from zero to that of the HCC. The field profiles for the combined matching and HCC section from one of the studies is

shown in Figure 9. The factor of two 6D cooling performance for this configuration is shown in figure 10. This factor is less than the factor of 8.3 for the hydrogen-filled or 6.5 of the helium-filled pre-cooling examples discussed above which have perfect matching since they follow a HCC decay section. The 6D cooling factor shown below is also less than the 3.7 of earlier studies because the length of the HCC has been reduced to fit in a smaller space and the matching is not completely optimized.

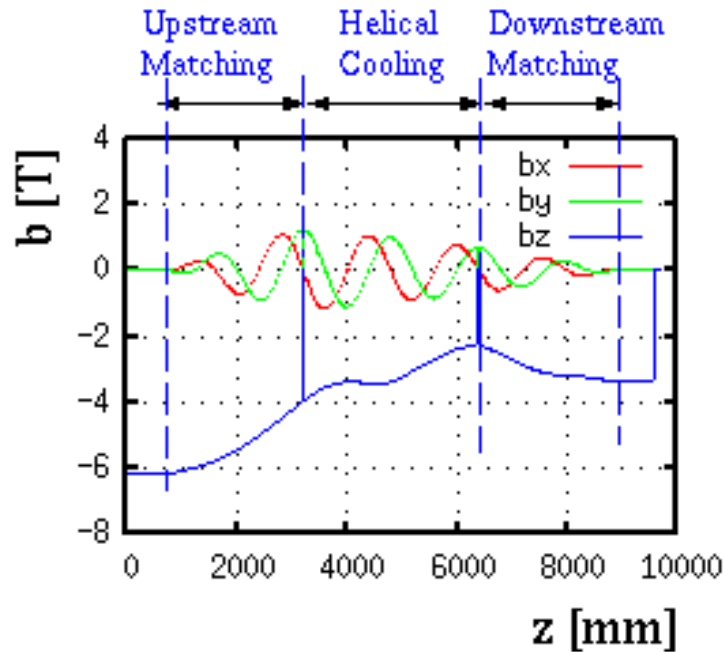


Figure 7 Field strength components along the reference orbit used in MANX cooling simulations.

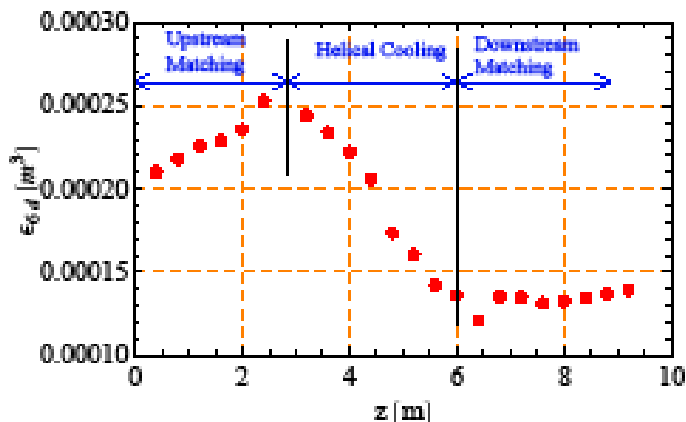


Figure 8. Emittance evolution in the MANX emittance matching and cooling sections as simulated in G4Beamline.

Although this matching scheme with a 1.5 period long phased-in helical channel is effective, it requires an additional 150% increase in the number of solenoid rings and infrastructure to mount them. There are two additional matching approaches that are currently being pursued as less expensive alternatives: The first is not to match at all and

orient the HCC channel so the beam from the MICE solenoids goes into the HCC at the 45° offset reference orbit. This configuration is shown in Figure 11. There are no losses upon entering the HCC from the upstream spectrometer since the acceptance of the HCC is 50% larger than the MICE spectrometer. There are significant losses upon exit from the HCC into the downstream spectrometer. The design is currently being optimized to reduce these losses. The second approach is to have a short 0.5 period matching section upstream and downstream of the HCC instead of the previously described 1.5 period matching section. This configuration shows no losses entering the HCC from the upstream spectrometer and loses only $\sim 5\%$ exit the HCC downstream. The latter may be a promising compromise with acceptable losses.

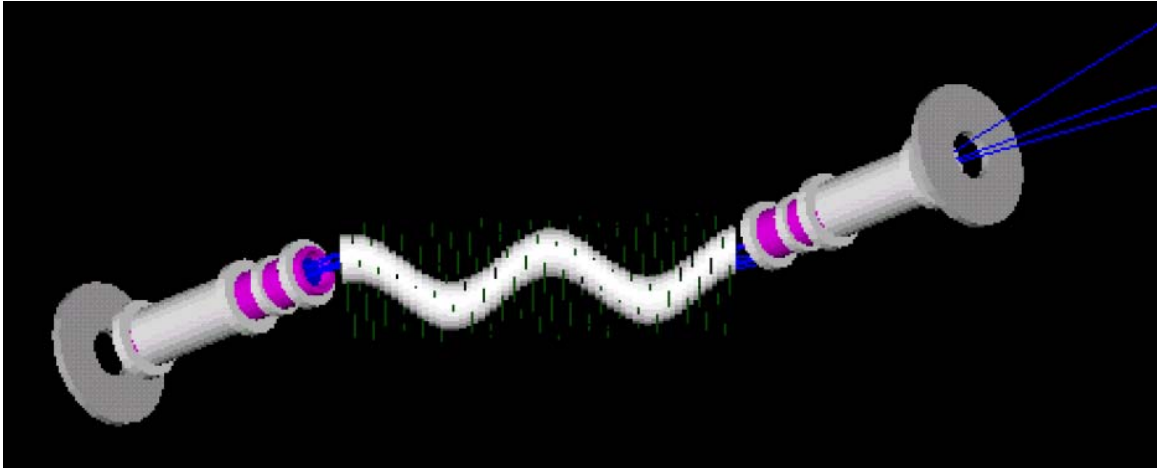


Figure 9 A G4beamline representation of the off-axis matching configuration where the HCC is placed at a 45° orientation to the MICE spectrometer so that the beam is oriented along the reference path at entrance into the HCC.

4 Experimental Method

MANX uses the same experimental method as MICE in that tracks are measured and emittances are reconstructed from ensembles of tracks. Much of the reconstruction and analysis software as well as the MICE spectrometers and other hardware can be used for MANX. The main differences between the two experiments are that MANX requires more precise measurement of the longitudinal momentum to determine the 6-d emittance and also desires measurement of the trajectories between the spectrometers to test the theory of the HCC and to understand losses. Also the initial beam momentum and energy loss in the channel are greater for MANX.

Studies of event reconstruction, selection and analysis strategies are in progress. We expect to benefit greatly from the experience that is acquired throughout the MICE phases, and we look forward to joining forces with the MICE collaboration to eliminate as much redundant effort as possible in analyzing the MANX data.

By measuring trajectories inside the HCC we will be able to reconstruct the emittance at a number of positions inside the HCC, and therefore be able to observe the evolution of the emittance reduction, and not just the overall emittance reduction. With a long cooling channel such as the HCC, there should be significant reductions of emittance at intermediate positions within the HCC. Studies have shown that the phase space projections evolve in shape as well as in size along the helical channel. It will be an important result to show that the evolution of the phase space patterns can be understood within the context of the Derbenev-Johnson theory.

As described in the following sections we plan to use state-of-the-art fast timing techniques to determine the longitudinal component of the momentum. Detectors inside the HCC also present technical challenges. We are considering two approaches – both using planes of scintillating fibers similar to those used for MICE. In one approach we would connect the scintillating fibers to clear fibers and bring the clear fibers out of the HCC to photon detectors, much as is done in MICE. The other approach is to interface SiPMs or other solid state photon counters directly to the scintillating fibers and possibly the readout electronics and bring electrical signals out of the HCC.

4.1 Definition of Baseline Configuration

The baseline configuration for MANX consists of all the elements of the MICE spectrometer reused, with the HCC replacing the cooling H₂ absorbers and RF sections of the MICE layout. In addition, the downstream spectrometer elements are moved further downstream to accommodate the longer length of the HCC, with its matching sections. We shall examine the individual elements of the MICE beam line and detectors to identify those elements that must be replaced or modified to meet the specific requirements of MANX. The baseline configuration includes matching sections upstream

and downstream of the HCC. Another configuration, without matching sections (the off-axis configuration), is being studied with G4beamline simulations. The possible installation of the configurations is described in section 8.2.

4.1.1 Conceptual View of Experiment Components

A generic diagram of the MANX experiment is shown in Figure 12. An incident beam of muons with momentum around 350 MeV/c passes through an upstream spectrometer where the trajectory, time, and momentum of each particle are measured. A matching section, which may be integrated with the spectrometer, then brings the beam to match the HCC acceptance. The beam then passes through a thin window that contains the liquid helium of the HCC. The beam passes through the liquid helium filled HCC where the momentum is degraded and 6D cooling occurs. The ~ 200 MeV/c beam exits the HCC through another thin window into the matching and spectrometer sections and is stopped in the calorimeter. Timing counters and Cherenkov counters in the spectrometer sections and the calorimeter at the end of the channel will be used for particle identification.

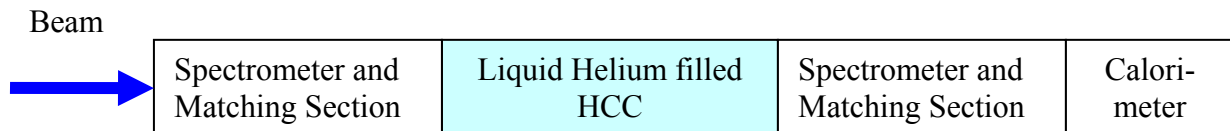


Figure 10 *Generic diagram of the MANX experiment*

The baseline spectrometer is based on solenoid geometry as is done in MICE. The matching sections then are designed for the MICE spectrometer type.

A more detailed diagram of the beam and spectrometer at RAL is shown in Figure 13.

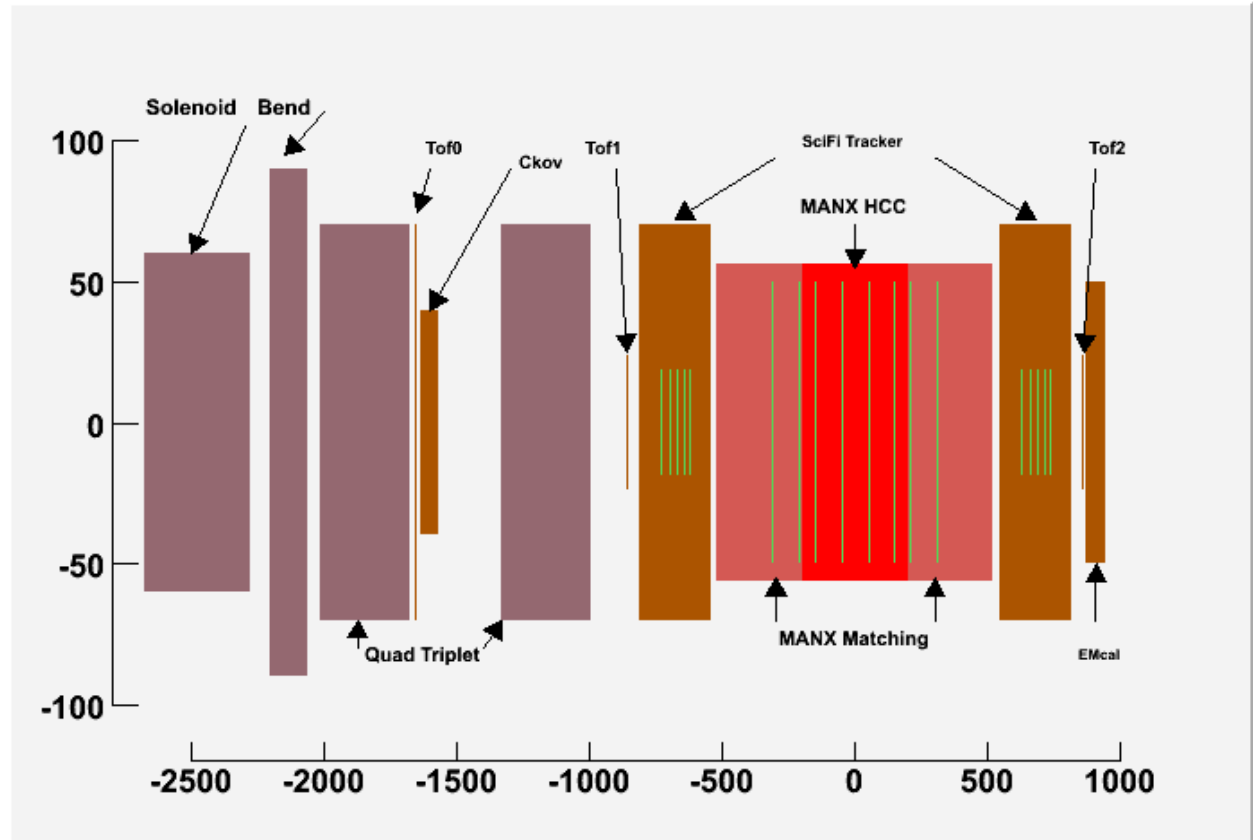


Figure 11 Sketch of RAL MICE muon beam line elements (violet) with MANX LHe-filled helical cooling channel (red) and evacuated matching sections (salmon) positioned between MICE spectrometers (brown). The decay solenoid is at the left. The dimensions are in cm.

The solenoid shown at the left is the decay solenoid, where pions decay into muons. (The upstream part of the beam from the internal target in the ISIS machine to the decay solenoid is not shown in the Figure 13.) The beam of muons then passes through a bending magnet for momentum analysis and two quadrupole triplets for focusing and beam shaping. Muon identification and rejection of pions and electrons in the beam is accomplished by the Cerenkov counter and a pair of time-of flight counters (TOF0 and TOF1).

4.2 Differences between MANX and MICE

The following is a list of differences between MANX and MICE. Details are provided in sections below.

- The incident muon beam momentum is higher: 350MeV/c vs 250 MeV/c in MICE. This impacts the beam tune, the muon rate, the pion to muon ratio, the

- identification of pions in the beam, and other areas. The higher momentum is required due to the amount of energy loss in the HCC.
- MANX requires a more precise longitudinal momentum resolution than in MICE. MANX is a 6D cooling experiment, whereas MICE is a 4D experiment, so MANX needs to measure the longitudinal emittance in addition to the transverse emittance. One approach is to determine the longitudinal momentum by means of improved time-of-flight measurements.
 - The MICE Cherenkov counters are designed for 250 MeV/c. For MANX the Cherenkov counters must be able to identify muons and reject beam pions and electrons at 350 MeV/c.
 - MANX requires the measurement of the emittance at a number of positions within the cooling channel. To be able to test the theory of cooling in the HCC it is important to measure the particle trajectories inside the HCC. It will also aid in identifying trajectories that are near the outer boundaries of the channel.
 - There may be differences in triggering and/or DAQ.
 - The MICE layout must be reconfigured to accommodate the MANX HCC and possibly MANX-specific detectors (and matching sections). In the MANX configuration in which matching sections are used, the MICE cooling and RF elements are removed and the downstream spectrometer and associated detectors are moved downstream to make room for the MANX HCC and matching sections. In the MANX “off-axis” configuration in which the matching sections are not present the downstream MICE elements must also be moved transversely.

We are currently reviewing and evaluating the MICE detectors in relation to the needs of the MANX experiment to determine which MICE elements need to be modified or replaced, and new detectors that are needed. The following sections treat specific technical areas that we have identified.

4.2.1 Beam Composition and Rates at 350MeV/c

The MICE beam line needs to be tuned for 350 MeV/c, the desired muon momentum. At this momentum the ratio of muons to pions is expected to be lower than at the MICE momentum of ~200-250 MeV/c. Work is in progress to calculate the beam characteristics at 350 MeV/c.

4.2.2 Improved Time-of-Flight Detectors

The time-of-flight counters in the MICE experiment, TOF0 and TOF1, have a time resolution of about 70 ps and are separated by 10 m. The resulting time-of-flight measurement is used for triggering on muons and rejection of pions in the beam, and for synchronizing with the RF phase, but is not precise enough to provide an accurate measurement of the longitudinal component of the momentum.

The momentum range of interest for MANX is from 150 to 350 MeV/c, where the dE/dx heating and the length of the cooling channel are acceptable. A sufficiently good velocity measurement could determine the momentum without the need for a magnetic spectrometer or it could aid the determination of total momentum for spectrometers

designed to measure transverse momentum. For example, 3.8 ps (13.2ps) change in the transit time of a 300 MeV/c (150 MeV/c) muon between two detectors separated by 1 meter corresponds to a one percent momentum difference.

The MICE spectrometers are based on solenoid fields, which match a 4D experiment, where transverse momenta are measured well. However, MANX requires that longitudinal momenta also be well measured. Simulations using G4MICE modified for MANX are just starting, to see if the present MICE spectrometers will work for a 6D experiment.

An innovative approach to improve the MICE spectrometers for a 6D measurement is to add very fast timing counters to measure the muon velocity. The University of Chicago (UC) and Argonne National Laboratory (ANL) groups are developing Time of Flight (TOF) counters with the goal of resolution better than 1 ps based on micro-channel plates with innovative anodes and electronics. A resolution of 5 ps may be sufficient for the total momentum measurement for the momentum range in which we are interested.

There are two interesting aspects of this idea that make it attractive to us. First, the UC effort is in need of help to simulate these devices using Geant4, a particular strength of Muons, Inc. Second, the UC effort is looking for a meaningful intermediate-sized project to develop the techniques of ps-resolution timing. Their ultimate goal is to make the measurement of 4-vectors, rather than 3-vectors, standard in large collider detectors, such as a next-generation 'CDF-III' detector at Fermilab, an upgrade to Atlas at the LHC, or a detector like the 4th Detector at the ILC. While that goal may require tens of square meters of fast timing detectors, a MANX application at RAL might need only one square meter. In November, 2008, Muons, Inc. and UC submitted a proposal for funding for development of fast timing counters.

4.2.2.1 Basic Concept of the Fast Counters

The exciting aspects of these fast counters are based on some recent innovations:

- The invention of a new method of making micro-channel plates that promises to yield better resolution and be considerably less expensive than current techniques.
- The ability to develop high-speed ASICs containing multiple channels of 40 GHz analog waveform sampling using switched capacitor arrays, thus greatly reducing electronics cost, power, and size.
- Simulations and tests of a strip-line readout that indicate an entire row of pixels can be read out with just two channels of electronics – this is a well-known technique, but applying it with bandwidths well in excess of 1 GHz is new, and permits a great reduction in electronics channel count, cost, complexity, and power.

The basic concept is shown in Figure 14.

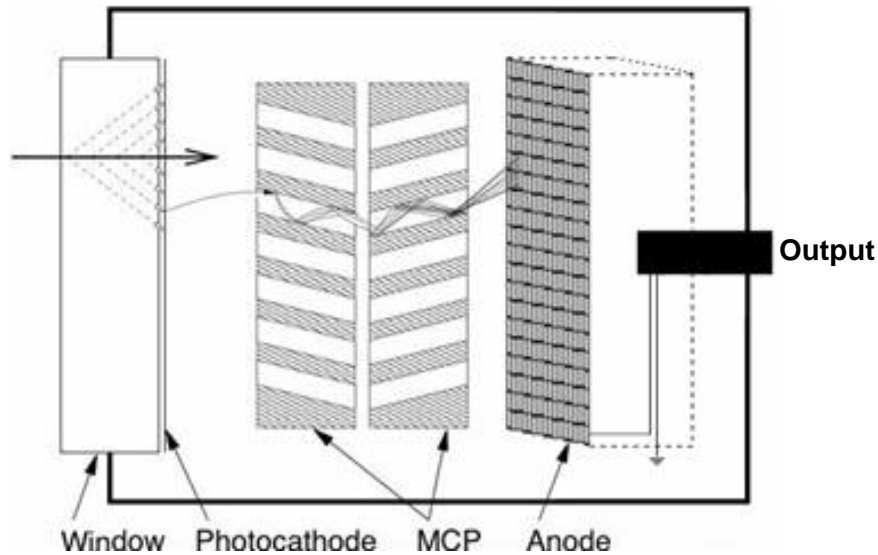


Figure 12 *Cross-section of the fast timing detector. A relativistic charged particle produces Cherenkov radiation in the window. This radiation is converted into electrons by a photocathode at negative voltage. The electrons are accelerated into and produce a shower in the micro-channel plates (MCP), and the shower is deposited on the segmented anode to be detected. Naturally this device is sensitive to photons as well (no Cherenkov radiator is needed); for high-energy photons a converter in front of the radiator can be used. Not shown: the anode has equal-time connections from each segment (pixel) to a transmission line, which has waveform-sampling channels on each end, giving both time and space positions. The drawing is not to scale.*

The entire package shown in Figure 14 is about 1 cm thick (along the particle axis, left-to-right in the figure), and the integrated-circuit readout electronics is mounted immediately behind it. By using modules formed of many internal multichannel plates made of anodic alumina functionalized with atomic layer deposition, this structure can be replicated to large areas with minimal dead zones at boundaries. The anode segmentation is determined by a printed-circuit pattern that is very flexible; the actual segmentation for a given application can be easily tailored to trade off requirements of cost, channel count, occupancy, and resolution. These planar detectors will be physically robust, which is important for commercial use, and will be able to withstand high pressures such as would be present in large water neutrino detectors. The detectors also do not need to be shielded or compensated for magnetic fields, a major advantage for many HEP applications and scanners for transportation security.

As the readout electronics is integrated with the detector module, the time resolution is not affected by the overall size of the detector – for each pixel the total signal path from the initial Cherenkov radiator to the readout transmission line is about 1 cm; the transmission line carries signals to waveform-sampling electronics on each of its ends. Detailed simulations give a signal band-width for a 2” transmission line (typical of a collider detector application) of 3.5 GHz; for a 48” module, the bandwidth drops to 1.1 GHz (still more than adequate for neutrino detectors and security scanners). Remembering that 1 ps corresponds to a distance of 0.3 mm at the speed of light, it is

clear that achieving ps resolution in a detector requires constraining the variance in the path lengths of light, electrons, and signals to be much less than a millimeter within the detector. That is not possible for traditional phototubes, but the few-micron pores of a micro-channel plate can do so.

4.2.2.2 Initial Test Results

Several aspects of this basic design have already been validated. For instance, the intrinsic time resolution of the Cherenkov radiator is quite good, as shown in Figure 15. Currently available commercial multi-channel plates (MCP) have almost adequate resolution, shown in Figure 16. The new anodic-alumina MCPs improve this, and new experiments are underway. Figure 17 shows that standard CMOS electronics using pulse sampling should be adequate. Further tests and experiments are underway.

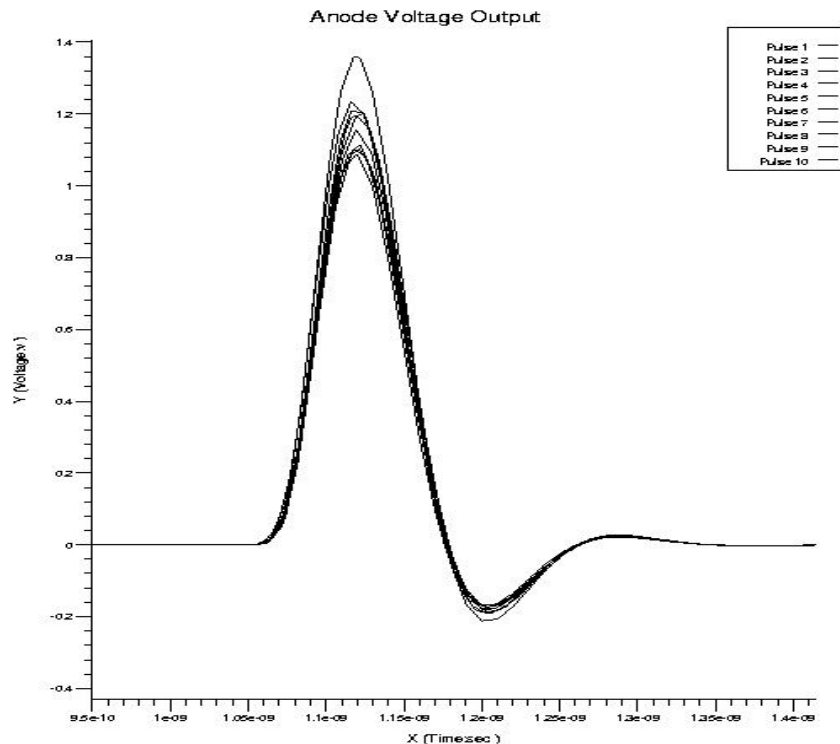


Figure 13 Simulation of Cherenkov light from a quartz window. For these 10 particles the jitter on the leading edge is 0.86 ps [19].

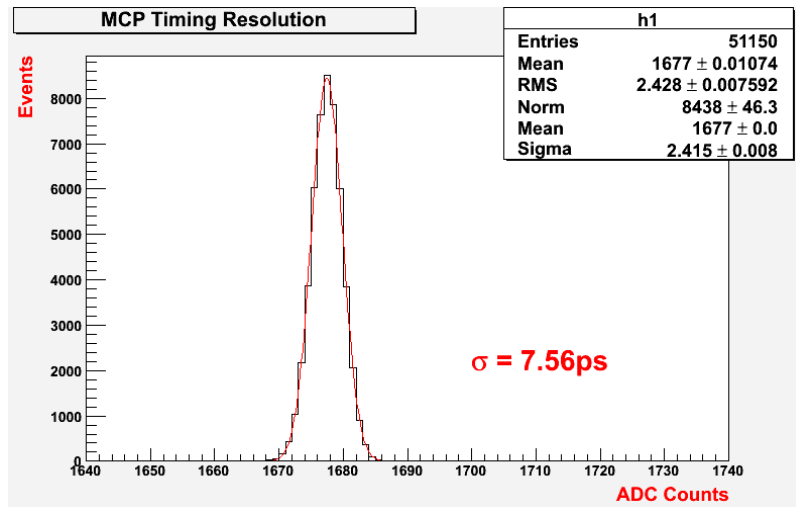


Figure 14 Measurement of the time difference between two commercial MCPs with $25\mu\text{m}$ pores. Data are for a 408nm laser with ~ 50 photoelectrons, at the laser test stand at Argonne (Hamamatsu PLP-10 picosecond laser and a commercial CAMAC readout electronics system). The intrinsic jitter of the system is $\sim 4\text{ps}$ and it has a resolution of 3.13ps [20]. The individual MCPs therefore have an intrinsic resolution about 4ps .

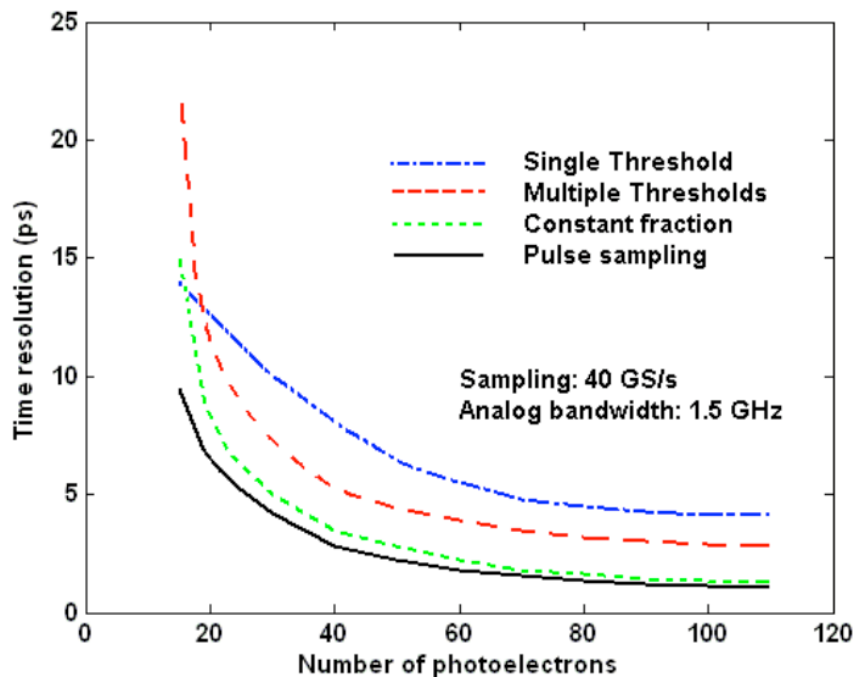


Figure 15 Electronics simulation of a CMOS multi-channel readout using various techniques. The analog bandwidth is 1.5GHz , and an 8-bit ADC sampling at 40GHz is used for the pulse sampling [21].

4.2.3 Detector planes inside the HCC

Measuring space points along the particle trajectory inside the HCC is an important capability for the MANX demonstration experiment, even though an actual cooling channel would probably operate without detectors inside.

4.2.3.1 Purpose of trackers inside the HCC

A record of space points along the trajectory enables study of the behavior of the particles as they lose momentum and scatter as they pass through the HCC. This helps test the underlying theory and the simulations. A further use of these measurements is to gain information about the trajectories of particles that do not make it all the way through the HCC to the external downstream spectrometer. Events can be taken with a trigger on particles that enter the HCC without requiring that the particle be within the acceptance of the downstream spectrometer. The HCC tracker gives information about the tracks that are lost in the HCC. Trajectories that are near the maximum radii are of particular interest for testing the theory. Having a record of the two transverse coordinates at several planes inside the HCC enables reconstruction of the “beam” profile along the HCC, which gives the ability to study the evolution of the shape of the muon distribution as the particles pass through the cooling channel. Additionally, trackers inside the HCC can be used as triggers, to enable selection of events that progress at least part way through the HCC. A variety of triggering modes can be implemented in the fast electronics. Furthermore, the interior tracking planes can be read out in an integrating mode to act as beam profile monitors inside of the HCC. In the early phases of the experiment it may be useful to operate the tracking planes in this mode, as diagnostics.

It is also possible to make a momentum determination of the particles inside the HCC. Although the particles lose momentum and scatter as they pass through the HCC, which makes momentum determination more complex, the upstream MICE solenoid spectrometer and time of flight yield the incoming momentum, and the downstream MICE spectrometer provides the outgoing momentum. With these constraints a fit can be made for the momentum at each of the intermediate measurement locations within the HCC. Inside the HCC there is a reference trajectory that remains a helix (ignoring scattering and straggling) about the HCC axis because the magnetic field decreases according to the energy loss. Particles with momenta higher and lower than the reference momentum have longer or shorter path lengths in the cooling medium, respectively, than the reference particles; however the tuning of the decreasing magnetic field is not as well matched to the energy loss. Thus, it is important to record space coordinates inside the HCC, to extract the best fit to the momenta inside, even with energy loss and a decreasing magnetic field in the HCC.

With the momentum vectors and space points at the measurement locations inside the HCC, the phase space distributions and the emittances can be computed at a number of planes inside the HCC. This information enables the study of the evolution of the emittance and the cooling function as the particles pass through the HCC.

The capability to measure the evolution of the emittance within the HCC is important in understanding the performance of the HCC.

4.2.3.2 Location of tracker stations inside the HCC

We propose to install 4 tracking stations inside the HCC, each consisting of 3 planes (u, v, and w), aligned at 120° angles, spaced at approximately equal intervals along the HCC axis, as indicated in Figure 19. We will undertake further simulation studies to determine if 3 coordinate planes are necessary in each station. In addition, we propose to install 2 tracker stations outside the HCC, one upstream and one downstream of the HCC. These would be useful to provide trajectory information in the regions in which the magnetic fringing fields are complex. From the standpoint of providing information along the trajectory, more tracking stations are better, but considering the amount of multiple scattering and energy loss straggling along the particles' trajectories, the gain may not be significant. For the MICE spectrometers the amount of material per station is 0.45% of a radiation length.

4.2.3.3 Type of trackers inside the HCC

Our baseline design is to use scintillating fiber trackers, similar to the ones used in MICE (and in the D0 Central Fiber Tracker). This will eliminate development time and reduce production costs. Each plane is designed to have a pair of scintillating fiber arrays, as shown in Figure 18, to provide good efficiency with minimal amounts of material. The fibers are plastic, 0.35mm diameter, mounted 0.427 mm apart in double planes, and grouped in sets of seven fibers per clear fiber and one clear fiber per readout channel, as indicated in Figure 18. To completely cover a 50cm HCC inner diameter requires 306 channels, each 1.63mm wide each containing 7 fibers (2142 fibers total). Each 3-plane station requires 918 channels, or a total of 3672 channels inside the HCC.

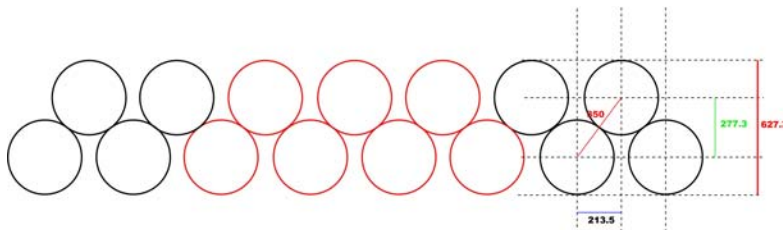


Figure 16 Arrangement of scintillating fibers in a tracker station plane (source: the MICE TR). The fiber diameter is 350 μ m, 7 fibers/channel, 1.63 mm/chan, which gives a resolution of 0.47 mm per plane. The fibers amount to 0.45% X_0 per double plane.

4.2.3.4 Methods to extract the tracker signals from the HCC

We are investigating a number of ways to bring out the signals from the fibers inside the HCC to be used in the data analysis, and possibly in the event trigger. The problem is more difficult than it is in MICE. In MICE the planes of fibers are in a straight-bore solenoid, so all planes are assembled as a single support structure, and the assembly is inserted into the bore of the solenoid. The HCC bore is helical, which makes insertion more difficult. Also the MICE solenoid bore is at room temperature,

while the interior of the MANX HCC is filled with liquid helium. This means that the signals must be brought out through the cryostat wall. If the HCC cryostat is built as a closed and welded structure then the tracker planes and any associated elements will be required to be permanently built into the cryostat. The signals from the detector will need to be brought out by means of feed-throughs. These constraints lead us to consider two possible configurations for the installation of the planes.

4.2.3.5 Tracker units within bore

One design for bringing the tracker signals out of the HCC is to adopt a method similar to the MICE trackers that are inside of solenoid magnets, that is, to splice groups of 7 scintillating fibers to a single clear 1-mm fiber and run the clear fibers toward the upstream (and downstream ends of the HCC). The clear fibers are attached to multi-fiber feed-throughs (MICE has 192 fibers per feed-through) that bring the signals out of the HCC. We would bring the fibers from the two upstream stations in the HCC out of the upstream end of the HCC and similarly the fibers from the downstream two stations are brought out of the downstream end of the HCC, as shown in Figure 19. Separating the upstream pair from the downstream pair simplifies the installation of the detector planes and reduces the space required for the clear fibers.

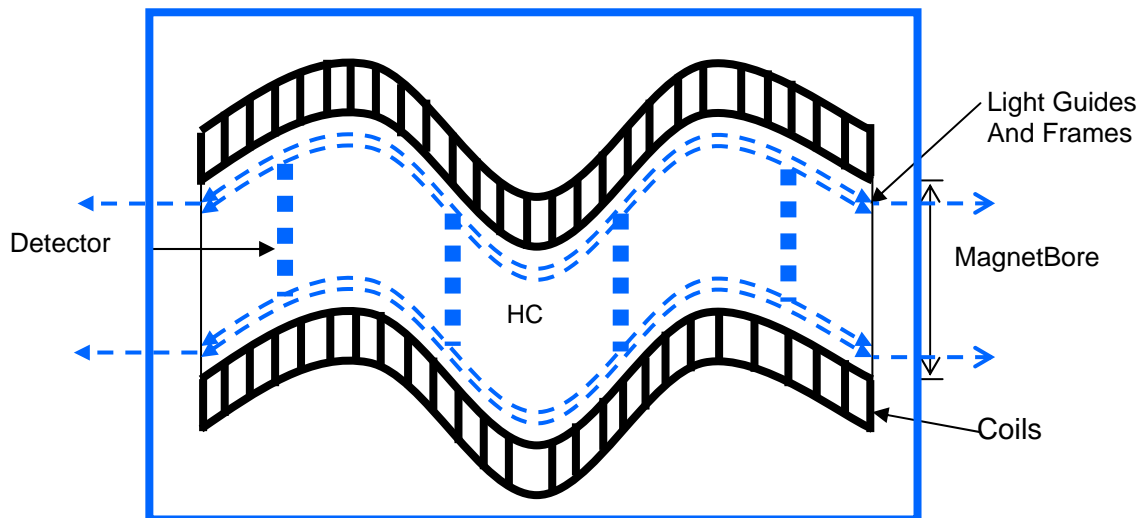


Figure 17 Schematic of placement of four tracker stations inside of HCC. There are also tracker stations upstream and downstream of the HCC, as indicated. Detector planes outside of the magnet are not shown.

Clear fibers are attached to the external connectors of the feed-throughs, and are attached to photon detectors outside of the HCC and away from the region of strong fringe fields. Our baseline design for the photon detectors is to use the same types as used in the MICE experiment, based on the D0 central fiber tracker: VLPCs and readout electronics. It may also be possible to acquire VLPCs and electronics from D0 after the Tevatron shuts down, which will reduce costs.

4.2.3.6 Tracker planes built into coil structure

The HCC solenoid consists of coil windings built into a supporting structure that serves several purposes: spacers for separation of the individual coils, displacing the positions of the centers of the coils so that the coil centers follow the desired helical path, and provision of mechanical strength to withstand the forces on the coils in the magnetic field. The tracker planes are mounted on specially designed spacers and built into the HCC assembly.

The advantages of this design are the following:

- The frames for the planes can be larger than the bore, so that the entire bore can be instrumented. In the baseline design the frames must fit within the bore.
- The clear fibers can be routed from the frames to the optical feed-throughs outside of the coils. In the baseline design the clear fibers are inside the bore, which introduces more material in the outer parts of the bore; the trajectories near the maximum radii are subject to scattering by the fibers in the bore.
- The fiber planes are built into the magnet structure and do not have to be inserted in the bore afterward.
- It may be possible to connect photon detectors such as SiPMs directly to the fibers inside the HCC. Perhaps the associated front-end electronics can be attached to the SiPMs, so that the digitized pulse-height information is brought out of the cryostat [22].

There are some disadvantages in this approach, e.g. when the planes are built into the coil structure they cannot be removed without disassembling the coils structure.

We present here a concept for the use of SiPMs and associated readout electronics. In Figure 20, we show a fiber plane that is attached to a supporting disk that can be mounted in the helical solenoid coil structure. Each group of fibers is connected directly to a SiPM and the readout elements are mounted on the support disk.

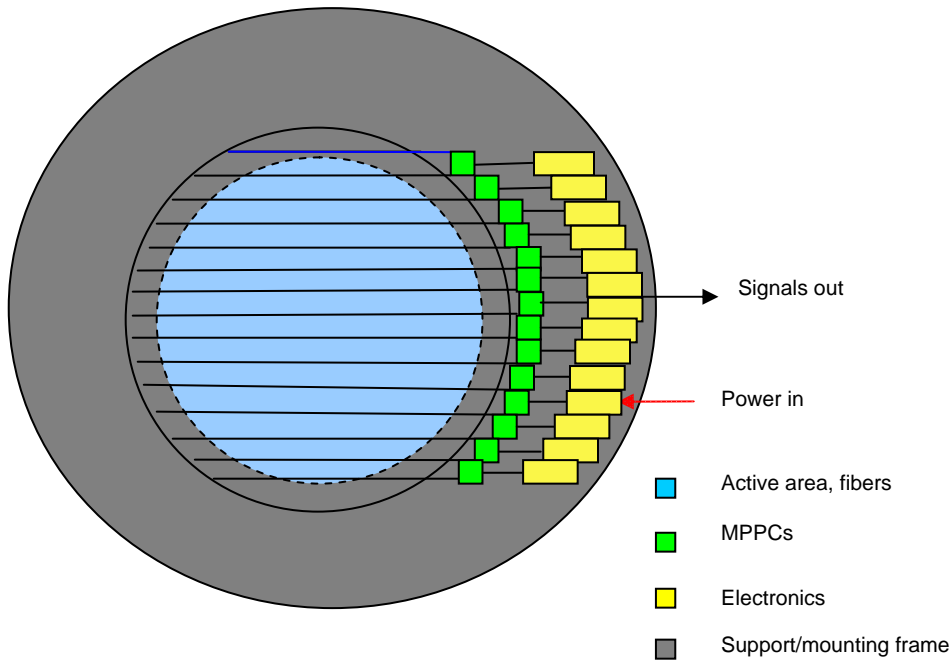


Figure 18 *Scintillating fiber plane and associated SiPM detectors and readout electronics on a mounting frame that can be built into the HCC coil structure*

A representation of the HCC with scintillating fiber plans mounted in the coil structure is shown in Figure 21, using SiPM-based detectors. Only electrical feedthroughs are needed. Feedthroughs shown are meant to be schematic – in an engineered version they could be mounted in other locations, for example at the end wall of the cryostat vessel.

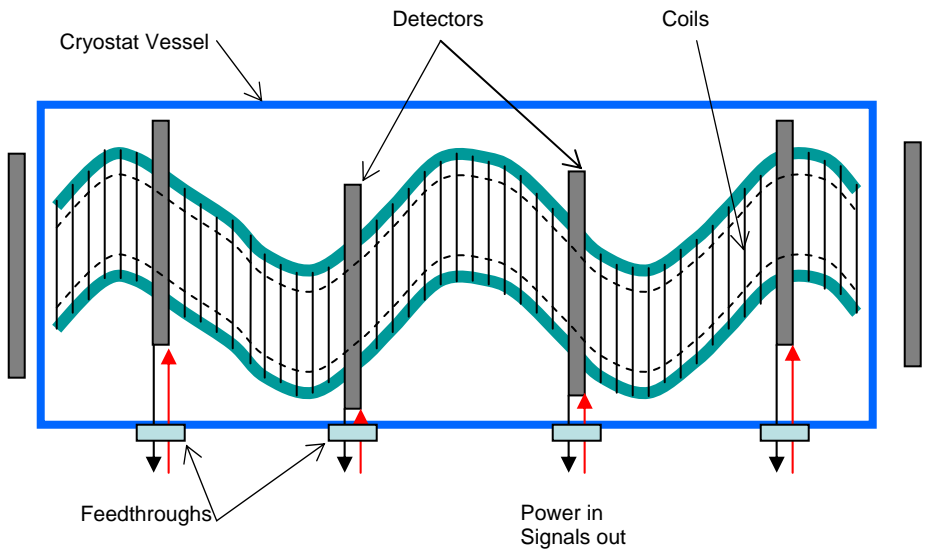


Figure 19 HCC with 4 tracker stations built into the coil structure. Detector stations upstream and downstream of the magnet are indicated.

4.2.3.7 HCC tracker development/testing issues

A number of issues need to be investigated and resolved concerning the use of scintillating fiber trackers in the HCC. The bore of the HCC is filled with liquid helium. It needs to be shown that the scintillating fibers produce sufficient light in that environment, and do not become stress-crazed due to the temperature range. Also the technique for constructing fiber planes must be such that the planes of fibers remain flat and intact in the He bath. They must also be able to withstand heating to room temperature and cooling to liquid helium temperature without damage to the fibers. Joints between scintillating fiber and clear fiber must be robust to withstand the temperature variations. Methods must be developed to be able to insert, align and position the tracking stations in the HCC.

We believe that fiber optic trackers will work in the LHe environment of the energy absorber. There already has been some prototype work to demonstrate this capability where we see that the scintillating fibers work well in LN₂, having no loss of signal or any indications of trouble with the bond between the clear and scintillating fibers. Some specific areas of investigation regarding scintillating fiber trackers inside the HCC are: possible reduction of light output of the scintillators at LHe temperatures, maintaining integrity of the spacing and alignment of the fibers in the LHe environment, interfacing with the design of the HCC such that detectors can be accommodated inside the cryostat, design of efficient feedthroughs/couplers for bringing the optical fiber signals out of the cryostat, selection of photo-detectors to convert the optical signals to electronic signals, and evaluating electronic readouts for processing the signals from the detectors.

There has been impressive progress recently in the development of SiPM (silicon photo-multiplier) technology [²³]. A number of companies have been producing commercial SiPMs, and the availability of new versions is growing. SiPMs consist of arrays of avalanche photodiodes (APD) and resistors on a single Si chip, where each APD corresponds to a pixel. Single photon quantum efficiency is near 100%, and because the APDs operate in the Geiger mode, each photon results in a standard signal from the corresponding pixel. Typical signals of multiple photons give rise to signals proportional to the number of photons received. The development of SiPMs is now focused on optimizing the designs to improve signal strength, reduce cross-talk, optimize the chip layouts to increase the active areas, reduce the noise levels, and improve quality and consistency of the units produced. Results from tests by particle physics groups have shown that SiPMs have good photon efficiency, are sensitive over a broad spectrum of light, are stable and have operated well in 4 Tesla magnetic fields, and are expected to work well in higher fields. SiPM costs are competitive with conventional PMTs, and their costs should decrease as production is commercialized.

4.2.4 Improved Particle Identification

4.2.4.1 Cherenkov Counters

The MICE experiment uses threshold aerogel-filled Cherenkov counters to reject pions and electrons. The radiators are designed for ~ 200 - 250 MeV/c, which is less than the

desired momentum of MANX (~ 350 MeV/c). However, one of the aerogel radiators that is being used at MICE is also suitable for MANX, namely that with index of refraction equal to 1.07 aerogel. For index 1.07 aerogel the threshold for muons is 275 MeV/c, while the threshold for pions is 376 MeV/c. Thus, pions with momenta less than 375 MeV/c will not produce a signal in the counter.

4.2.4.2 Calorimeters

We are evaluating the performance of the rejection of electrons downstream of the HCC. The NIU group, which has experience in calorimetry, will provide calorimeters designed for the MANX experiment, if needed.

.

.

.

5 Requirements for Measurements

5.1 *Statistical Precision Needs*

The amount of cooling anticipated for the HCC is considerably greater than that expected for the MICE cooling sections, about a factor of 2 reduction vs about 15% for MICE. A rough estimate is as follows. Based on the relative cooling factors the number of events required to determine the cooling at MANX to the same relative precision as MICE is about a factor of 100 less than at MICE. Measurement of the characteristics of the cooling of the HCC will require study of events near the limits of the acceptance of the HCC, which will require selection of sub-samples of the data. To get adequate statistics on selected regions will require additional data. More detailed studies of the statistical precision required to determine the emittance reduction performance of the HCC will be performed. The MICE experiment loses 90% of its beam due the need to select beam spill segments that are synchronized with the RF timing of their RF cavities. MANX has no RF so it can use the entire spill.

5.2 *Systematics and Ancillary Measurements*

The mapping of the magnetic field of the HCC magnet and the matching sections, if used, will be done at Fermilab.

Studies of systematics of the detectors and spectrometer will be done as part of the simulations, and in conjunction with systematics that are determined by the MICE experiments.

6 Beams

6.1 *MICE Beam Line*

The elements of the MICE beam line are shown in Figure 22. The target plunges into the ISIS beam, a quadrupole magnet triplet captures pions produced in the target, which are bent by a dipole magnet and pass into the MICE Hall, where they enter a decay solenoid. Muons of the desired momentum are selected by the second dipole magnet, and transported to the MICE upstream solenoid spectrometer. The MICE cooling sections and downstream spectrometer and detectors are not shown. A Pb diffuser is used to scatter the muons to increase the initial emittance of the beam to about 2π to 10π m-mrad, depending on thickness of the Pb diffuser.

The MICE beam line was designed for a muon momentum of 220 MeV/c, but it can be run as high as 400 MeV/c, which is suitable for a MANX beam momentum of 350 MeV/c. The composition of the beam at 350 MeV/c has not been determined as yet.

The MICE beam has the following time structure [24]: MICE gets about 1 beam spill per second, depending on the allocation of spills from the 50 Hz ISIS rate. The expected rate

is about 600 muons per 1 ms spill, in the MICE momentum range of 140MeV/c to 240 MeV/c, with an internal fine structure due to the ISIS 3 MHz RF frequency.

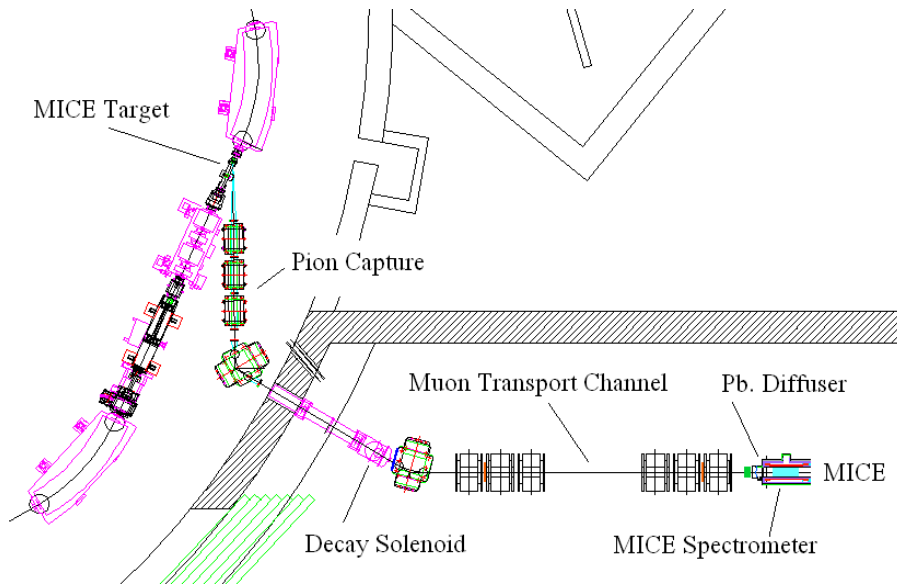


Figure 20 MICE beam line at RAL (From the MICE TR).

6.2 Test Beams at Fermilab

There are two test areas at Fermilab that will be available for MANX testing – the MuCool Test Area (MTA) and the Meson Test Beam facility (MTBF). The MTA has a beam from the Linac of 400 MeV protons, with short spills of ~ 25 nsec to ~ 100 μ sec at a rate up to 15 per second. The MTBF beam is based on the Fermilab Main Injector beam of 120 GeV protons and a secondary target that can produce positive and negative beams from ~ 1 GeV/c to 120 GeV/c. There is now a secondary target that produces a low momentum tertiary beam of 200-400 MeV/c, initially for the testing of MINERVA calorimeters.

The beam has a long spill time of 1-4 seconds, with a rep rate of once per 1-2 minutes. Beam intensities vary depending on beam momentum and sign. Beams of $\sim 10^6$ protons per second at 120 GeV/c are available and rates are a few thousand per second at low energy.

The MTA beam is dedicated to muon cooling experiments such as the effects of beams passing through RF cavities, and operation of RF cavities in a magnetic field. It could be used for testing of MANX detectors.

The MTBF is a test facility that is available for any users, after approval of proposals. Groups have used the facility for a wide range of testing activities from very short runs of a few days to long term testing programs such as those of the CALICE calorimeters. The high energy primary and secondary beams can be used for testing of the TOF and scintillating fiber planes, and low energy tertiary beam is particularly well suited to test pion and muon identification in the low energy region corresponding to the MICE beam energies.

7 Simulations of Baseline Beam/Detector Configuration

We plan to use G4MICE to simulate the MICE beam operating at 350 MeV/c. The rates and beam composition are expected to be different than at 220 MeV/c, the design momentum. The higher momentum pions decay at a slower rate, so we expect a somewhat lower muon rate and a higher pion-to-muon ratio. Another difference is the relative production of higher momentum pions produced in the ISIS target. We are also very interested to learn how the measured MICE beam rates compare to the calculated and simulated rates.

We have begun to enhance the G4beamline program to incorporate the full MICE beam and detectors, and to include MANX channel types for a complete end-to-end simulation of MANX using the G4MICE program.

8 Components Currently Available and Needed

8.1 Helical Solenoid and Matching Sections

These components are to be provided for MANX. Details are contained in other sections.

8.2 Existing MICE Configuration and Adaptations Needed for MANX

The complete MICE layout in the MICE Hall at RAL is shown in Figure 23, including ISIS magnets and target, the MICE beam line elements, and the MICE components. Of particular note is the amount of space between the MICE solenoid spectrometers and the amount of space between the electron calorimeter and the beam stop. The downstream end of the upstream spectrometer is at about 10 m on the metric scale in the figure, and the upstream end of the downstream spectrometer is at about 17 m on the scale, which indicates that there is about 7 m available for the MANX HCC if the MICE cooling channels were removed.

From Figure 13 the space required for the HCC and matching sections is about 10 m, with 6 m required for the matching section and about 4 m required for the HCC. Thus, in a version of MANX without matching sections the MANX apparatus could fit into the space made available by removing the MICE cooling sections, and the downstream spectrometer and calorimeter need not be moved downstream. (The optimal position of the downstream spectrometer would probably be immediately downstream of the HCC.) With matching sections it would be necessary to move the downstream apparatus about

3 m downstream. It can be seen that the space between the last element of the MICE layout and the shielding at the end wall of the MICE Hall is about 4.5 m, which accommodates a 3 m move of the apparatus.

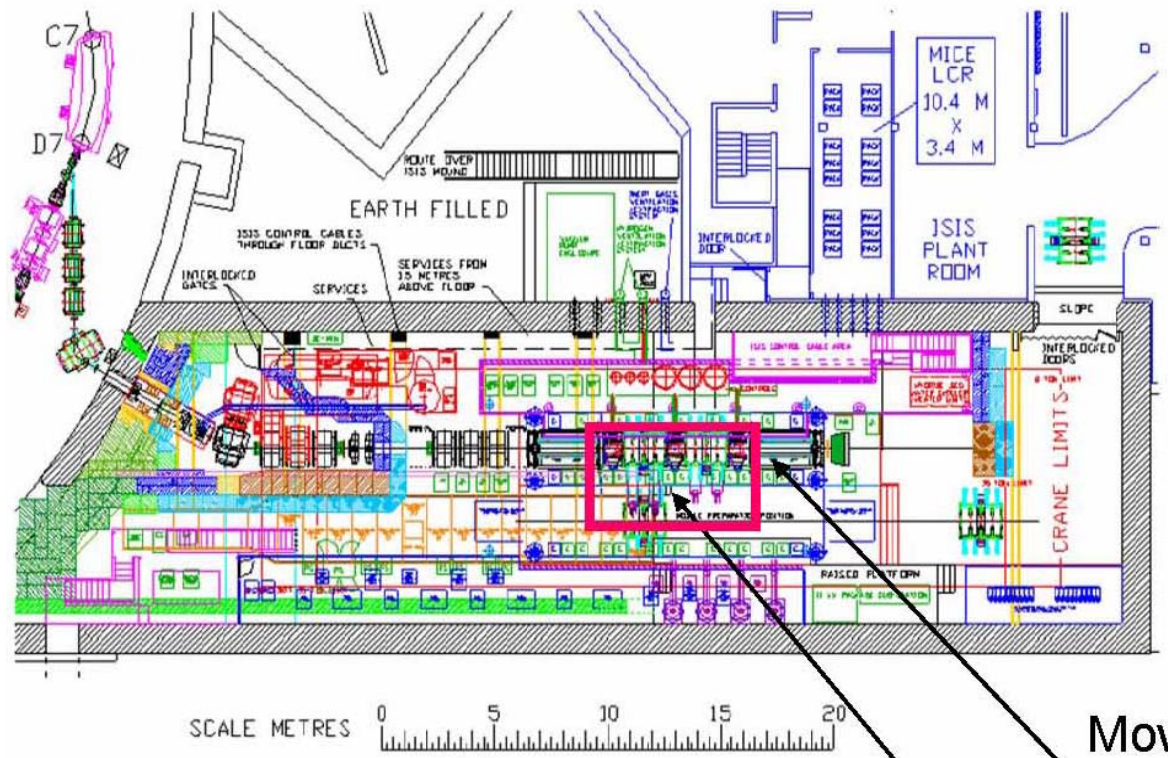


Figure 21 Layout of MICE experiment at RAL, showing complete Step VI arrangement with three cooling sections and the associated RF stations. A section of the ISIS accelerator magnets is at the left, with the MICE beam line quadrupoles and first bending magnet outside the MICE Hall.

For the MANX channel as shown in Figure 11, in which there are no matching sections, but the HCC is placed at a 45° angle so that the beam enters aligned with the reference trajectory, space required along the beam line is about 3 m but the downstream emerging beam line is displaced by about 3 m to the upstream beam line. This requires that the downstream spectrometer must be moved transverse to the upstream beam line. It appears that there is about 3m of space to the right of the beam, which would accommodate the HCC and the relocation of the spectrometer. These are very rough feasibility assessments and all aspects have not been included. For example, additional space needed for the HCC cryostat (which has not been designed) is not considered.

8.3 Software

The existing and expected refinements and developments in software for MICE represent a rich resource that can be used by MANX. The simulation, data acquisition, track reconstruction and analysis functional packages will have been used throughout the MICE project, and will be of direct use to the MANX experiment. Several of the current MANX groups are already working on MICE software and will continue to do so through

the MANX era. We anticipate that groups from the MICE collaboration will join the MANX collaboration and continue to upgrade and support the evolving software.

The main additions that will be needed to upgrade the software for MANX are for the detectors inside the HCC, track fitting along the trajectory in the HCC, matching to the tracks in the existing spectrometers, and the determination of the longitudinal momentum component from the TOF information.

Additional DAQ software will be required for readout of the ps TOF counters and the detectors inside of the HCC and integration into the overall MICE DAQ.

The MICE analysis package will be augmented to incorporate the HCC and TOF information.

9 Schedule, Resources Needed, and Cost

9.1 Boundary conditions

MANX should not be installed until MICE has achieved its objectives. It also would be unfortunate to have a long break after MICE finishes and before MANX begins since the expertise of people and equipment tend to disperse and deteriorate. Ideally, the MANX apparatus should be ready to take data about a year after MICE is done. This is enough time to install the HS magnet, interface it and new detectors to MICE, and tune the beam to new requirements.

9.2 MICE Schedule

At the recent MICE collaboration meeting in October, 2008 [25], the MICE “aspirational” schedule shown in Figure 24 was presented. MICE is planned to proceed as a series of steps leading to a full complement of apparatus, with three hydrogen absorbers, two solenoid spectrometer trackers and particle identifiers. The following list enumerates the characteristics of the steps.

- I. Step I includes setting up the beam, the beam monitoring counters, and the decay solenoid. Currently in progress, expected completion Spring 2009.
- II.
- III. Step II adds the first solenoid spectrometer and TOF2 counter, scheduled for spring of 2009.
- IV. Step III adds the second solenoid spectrometer, a solid absorber, and downstream particle ID detectors, planned for summer and fall of 2009.
- V. Step IV replaces the solid absorber with the first liquid hydrogen absorber, planned for fall of 2009 until spring of 2010.
- VI. In Step V the first of the RF stations and the second hydrogen absorber are installed and expected to run in spring of 2010.

VII. In Step 6 the complete setup, with two RF stations and three hydrogen absorber units, is planned for late 2010 and into 2011. This is the final step of the MICE program.

Following the completion of Step 6, the MICE collaboration has indicated that they desire to maintain the facility and make it available for additional studies and measurements. The earliest time for doing the MANX experiment in RAL as an extension of MICE is after Step 6, approximately 2011.

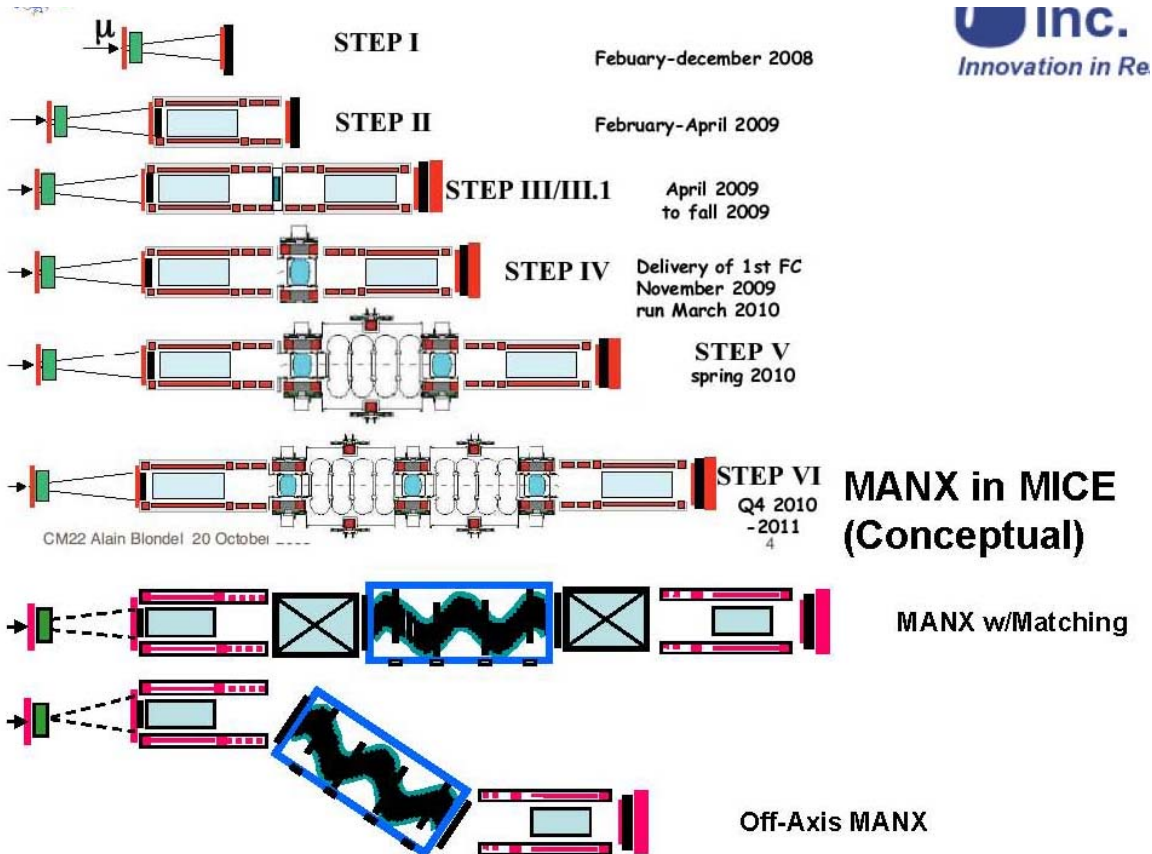


Figure 22 Representation of the MICE schedule

9.3 Completion of HCC and Matching Sections

The four-coil model has been completed and the field mapping is underway at Fermilab. An estimate of the time required to build the full HCC magnet, without considering RF cavities or detectors in the design, was presented at the July, 2008 MANX meeting [26]. The time estimate, which included specification, engineering, cryogenics, procurement, fabrication, assembly and testing, was approximately four years for the HCC magnet, and did not include the matching coils. A decision on whether to build matching sections is required at the specification stage. Based on this estimate, if the HCC construction project were to begin in spring, 2009, the magnet would be completed in spring, 2013. The cost was estimated to be approximately \$6M. Whether the magnet development group at Fermilab may be able to start working on the HCC as early as we desire depends

on other magnet projects being undertaken and priorities to be determined by the Fermilab administration.

The MANX collaboration plans to submit a proposal to the Fermilab Accelerator Advisory Committee (AAC) in January, 2009 to request support for building the HCC and other items for MANX, based on the plan to run the experiment at RAL as an extension of the MICE experimental program.

9.4 Responsibilities of Participating Groups and Needs from Fermilab Divisions

The mode of operation of Muons, Inc. is collaborative, by the nature of its funding. Muons, Inc. will provide enhancements to and support for G4beamline with its grant with IIT. The TOF project is a joint effort between Muons, Inc. and the University of Chicago. The development of detectors and electronics for the HCC detectors is a collaborative effort of Muons, Inc., Northern Illinois University and Fermilab. The HCC magnet development has been a joint effort of Muons, Inc. and Fermilab. The other participating groups will contribute to hardware, software, and electronics areas as the project proceeds. We are also seeking to participate more actively in MICE experiments, and are also seeking additional collaborators from the current MICE participants as well as additional groups. We anticipate that the collaboration will grow more rapidly after the proposal is approved.

The specific needs from Fermilab will be elucidated in more detail in the proposal to the Fermilab AAC. However there are several Fermilab Divisions that could support the effort. The Technical Division has been the major player in the design, construction, and testing of the HCC magnet. The Research Division facilities and support will be important for scintillator plane development and construction, as will the electronics department design facilities for the design of front-end electronics for the detectors in the HCC. Individual members of the Accelerator Division will surely join the collaboration and contribute in their related technical areas.

The Northern Illinois University group has indicated an interest in providing an improved electron identification calorimeter for the downstream region and has graduate students who are working on beam-related and analysis issues.

The IIT group has one post-doc who is working on the muon beam simulations. Both NIU and IIT are likely to have students on the experiment.

The Jefferson Lab collaborators have worked on the fundamentals and systematics of muon cooling and will continue to support the planning, analysis, and interpretation of the data.

9.5 Completion of Additional Components Needed for MANX

The two major Detector developments/additions for MANX are the ps time-of-flight detectors and the detectors inside the HCC. These could be developed and built with

support from the SBIR Phase 1 (9-month) and STTR Phase 2 (2-year) grants. Additional support from other collaborators is likely to be provided.

9.6 *Timeline for Building, Testing, Installing and Running the Experiment*

Assuming that the schedule for the construction of the HCC magnet requires the longest preparation time, the transport of the equipment to RAL could take place in early 2013. This fits in well with the conclusion of the present MICE program in 2012. In broad terms the magnet could take 4 years and the detectors 3 years. There is approximately one year after the completion of MICE for the MICE apparatus to be reconfigured to permit installation of the MANX equipment. Following this we anticipate about 2 years to install, test, and run the MANX experiment.

9.7 *Cost Estimate*

The major cost item is the HCC magnet, about \$6M. We plan to provide a more complete cost estimate in the updated version of the proposal to be submitted to the Fermilab AAC in January.

The cost items for RAL include reconfiguring the MICE apparatus to accommodate the MANX equipment, installation costs, and costs of operating the MICE beam and facility for approximately two years for the duration of the MANX startup and data taking.

The cryogenics needed for the MANX magnet will be discussed in view of expected RAL capability and the design optimized accordingly.

9.7.1 *Scope of Estimate*

(To be completed later.)

9.7.2 *Estimate Methodology and Basis*

(To be completed later.)

9.7.3 *Contingencies*

(To be completed later.)

10 MANX and Other Muon Collider and Neutrino Factory R&D

10.1 *Relationship to the Muon Accelerator R&D 5-Year Plan*

The Fermilab Muon Collider Task Force (MCTF) was established in 2006 to develop a plan for a program to advance the technologies necessary for a possible energy-frontier muon collider (> 1 TeV) at Fermilab. Many of the concepts and technical elements of

this proposal were included in the Muon Collider Task Force Report [27], co-authored by most of the MANX collaboration as well as groups from Brookhaven, LBNL, UCLA, and U. of Mississippi. The high pressure RF studies, the helical solenoid magnet work, high temperature superconductors, and the cooling studies that relate to MANX are described in the report. The proponents of this proposal are in close contact with the MCTF, and our plans are well known to the MCTF.

Recently the MCTF and the Neutrino Factory/Muon Collider Collaboration (NFMCC) have started work on a 5-year plan [28] which has been presented to the Department of Energy for funding. The 5-year plan is directed toward delivery of a Muon Collider Design Feasibility Study Report (MC-DFSR) and participation in the preparation of a Neutrino Factory Reference Design Report (NF-RDR) in 5 years. It does not address other uses of muon beams, such as intense stopping muon beams for studies of rare processes, e.g. the muon-to-electron conversion ($\mu 2e$) experiment, which recently was granted Stage I approval at Fermilab. In the section relating to 6D cooling, the draft plan discusses the HCC as one of three schemes under consideration, and it does not advocate a particular choice. There is also a discussion of the MICE experiment and its relationship to a neutrino factory.

The 5-year plan supports the development of the MANX proposal but does not request funding for the experiment itself within the 5-year time frame. The plan proposes to ramp up the effort and funding for a muon collider technical program. As such, the plan outlines a program of building several short helical solenoid sections that can be used to study the operation and integration of RF with the sections of coils, and designing a hydrogen gas-filled HCC that has integrated RF cavities. A 6D test with beam would come later, after the time period covered by the plan.

We believe that doing the proposed MANX 6D cooling experiment with helium absorber and without RF will further the goals of the MCTF and NFMCC and will provide a meaningful test of cooling principles. It will also lay the technical groundwork for designing useful cooling channels for stopping muon beams.

In short, we believe that MANX is an essential complement to the Muon Accelerator 5-year Plan. To the extent that it can be supported by people and funds that would not otherwise be used on the 5-year Plan, MANX is much more than just aligned with the Plan in that it is a valuable addition.

Muon accelerator science and technology will be advanced by adding resources from other countries and other US institutions that will join an interesting 6D cooling experiment, but not necessarily a Fermilab study. For example, several universities have joined in this proposal and we anticipate more of them will join in the coming year. These university people from the high energy physics world not only have the right background for MANX, they also are the ones to energize their community and make it aware of the excitement of a muon collider.

MANX as part of the MICE program will attract a larger group of collaborators, with valuable equipment and well-matched expertise, to both MICE and MANX. This is an extraordinary opportunity.

10.2 Relationship to MICE

Several of the MANX collaboration members and institutions are already participating in MICE. It would be natural for them to continue this work by doing MANX at RAL, instead of mounting a separate experiment at a different facility. It is a mutually beneficial association – the MICE experiment would benefit by having additional participation by the MANX collaborators, and the MANX collaborators would be able to save a great deal of effort and cost by using the MICE beam, experimental hardware and software. It also benefits the MICE program and RAL by extending the return on the investment to do additional physics and make further technical advances.

Appendix A . Development program for high pressure RF cavities

High Pressure RF and the Continuous Absorber Concept

Filling RF cavities with gas is a new idea for particle accelerators and is only possible for muons because they do not scatter as do strongly interacting protons or shower as do less-massive electrons. Although the MANX experiment supports the use of a HCC filled with hydrogen-filled RF cavities, the experiment itself does not require RF cavities and, in addition, also supports an alternative to the gas filled RF cavity approach to 6D cooling, where HCC sections much like MANX would alternate with sections of conventional evacuated RF cavities.

Experiments are underway at the Fermilab Mucool Test Area (MTA) to test the concept of RF cavities pressurized with hydrogen gas. A test cell has been constructed, as shown in Figure 25. The test cell has two hemispherical electrodes, which can be made of various materials. Tests have been made of Cu, Be, W, and Mo thus far. The cell can be pressurized up to 1600 psia at STP, and can be operated at 800 MHz.

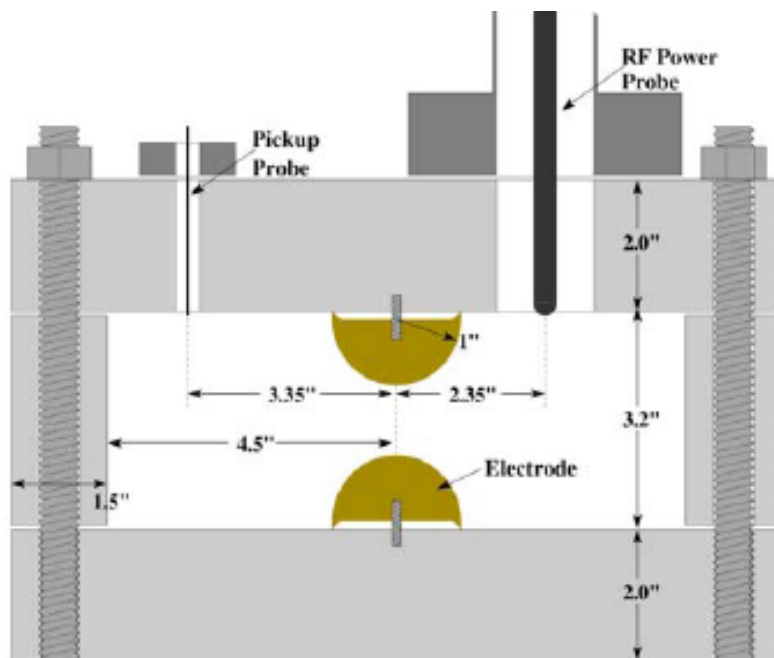


Figure 23 High Pressure Gas-filled RF Test Cell

The results of tests of the test cavity filled with hydrogen gas are shown in Figure 26. As the pressure increases, the mean free path for ion collisions shortens so that the maximum gradient increases linearly with pressure. At sufficiently high pressure, the maximum gradient is determined by electrode breakdown and has little if any dependence on pressure. Unlike predictions for evacuated cavities, the Cu and Be electrodes behave almost identically while the Mo electrodes allow a maximum stable gradient that is 28% higher. The cavity was also operated in a 3 T solenoid magnetic field with Mo electrodes (magenta); these data show no dependence on the external magnetic field, achieving the

same maximum stable gradient as with no magnetic field. This can be compared with measurements of 805 MHz evacuated cavities that show the maximum surface gradient is reduced from 50 MV/m to about 15 MV/m at an external magnetic field of 3 T.

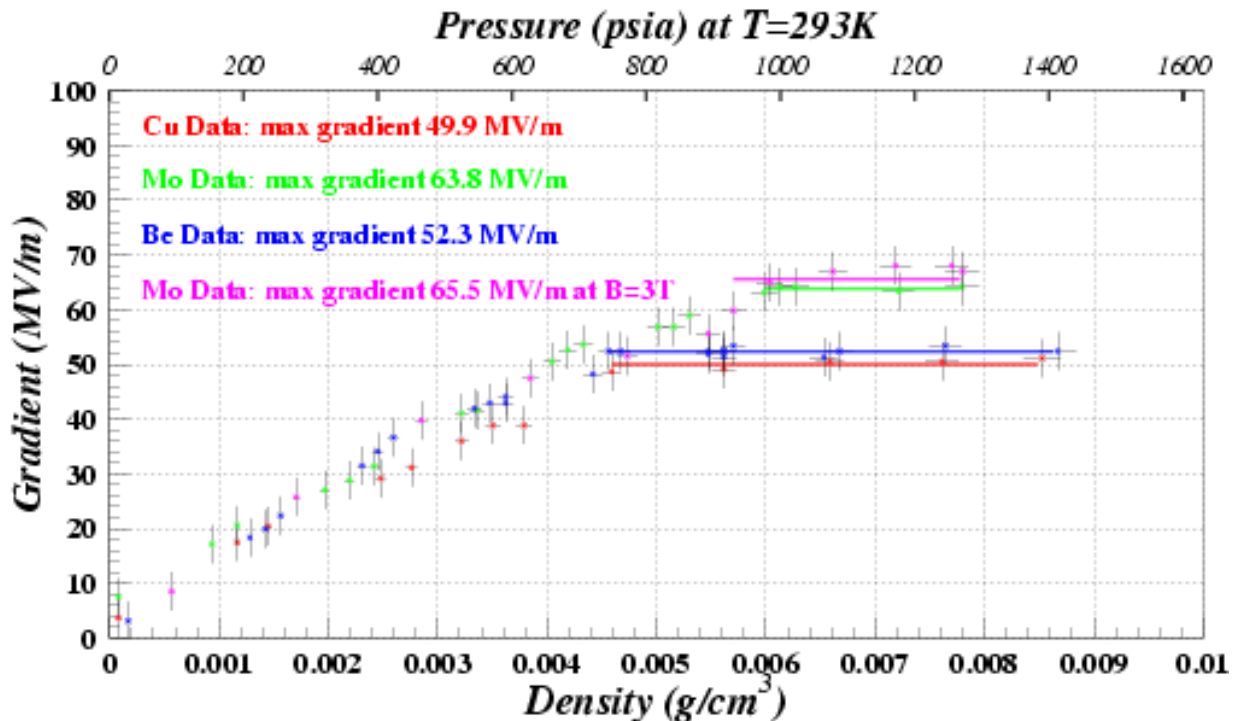


Figure 24 Measurements of the maximum stable Test Cell gradient as a function of hydrogen gas pressure at 800 MHz with no magnetic field for three different electrode materials, copper (red), molybdenum (green), and beryllium (blue)

Figure 26 displays results from tests at the MTA that show that pressurized cavities have an advantage over usual cavities that operate in vacuum in the strong magnetic fields that provide the strong focusing required for effective beam cooling. In a 3 Tesla field, the maximum stable gradient of the Muons, Inc. 800 MHz test cell showed no maximum gradient degradation, while an evacuated cavity had reduced performance under similar conditions. Additionally, the dual use of the real estate for energy absorption by the hydrogen and for energy regeneration by the RF cavities can be an important feature for cooling channels requiring the highest muon flux where the muon lifetime is relevant.

The next important step will be tests of the pressurized RF test cell in an intense radiation environment. A 400 MeV proton beam line is being installed in the MTA and an experimental program to develop pressurized RF suitable for operation in a muon cooling channel should start soon. In addition to the test cell used for the measurements in Figure 26, a new pressurized RF cavity is being designed, which will be more like a conventional cavity with new features to mitigate breakdown and tune changes that may be caused by the bright beam in a muon cooling channel.

Appendix B Four-Coil Model of Helical Solenoid Magnet

The MANX collaboration is working with the Fermilab Technical Division to design and engineer the HCC and emittance-matching magnet systems, including construction and testing of a four-coil demonstration magnet for the superconducting helical solenoid.

The four-coil demonstration magnet has been designed and constructed, and is currently set up for magnetic measurements at Fermilab in the Dewar of the Technical Division Vertical Magnet Test Facility (VMTF).

The status of the project has been presented at a recent conference [29]. Figures in this section are from the conference report.

This program will have many benefits to the MANX program to build a full scale helical cooling channel.

First, the tooling to make the coils and the coil manufacturing procedures of the engineering design will be directly applicable for the full scale MANX solenoid. The coil manufacturing process is a major time and cost driver for the full scale magnet and the 4-coil test will thus reduce the uncertainty and required contingency in the final project.

Second, the mechanical support structures and the measuring system for the 4-coil test are directly applicable to full scale MANX. The mechanical structure is designed to withstand the forces from adjacent coils, with the end coils likely having the largest asymmetric forces. In the central part of the HCC magnet channel the coil forces are largely radial, whereas there are significant longitudinal forces near the ends of the magnet channel that must be supported.

Finally, these coils can be used to do magnet studies that would be too costly or involve too much program risk for the full scale magnet. Studies include quench protection, complicated by strong field coupling of adjacent coils, and powering schemes for individual coils to compensate for the required momentum or z dependent field variation due to dE/dx loss. It is also possible to safely study the magnet response due to certain error conditions such as quench detection failure. We will design the support structure so that the center coils of the 4 coils will be easily replaceable, allowing QA tests of production coils for the full scale MANX Helical Solenoid.

Plan Details: Figures 27 and 28 show a schematic of the 4-coil test geometry. The coils are modular and will operate in liquid helium.

Coil design manufacturing: Existing NbTi cable from the Fermilab cable inventory was used. Tooling was designed to wind the cable on a stainless steel mandrel. Detailed mechanical/field calculations guided the design of the coil mechanical structure.

Support structure: The support structure will be designed to accommodate the expected 300 kN longitudinal forces and ~200 kN transverse restoring forces. The dewar dimensions are approximately 600 mm in diameter and 4000 mm in length. Coil offset is accomplished by mounting the rings perpendicular to the gravity/dewar axis.

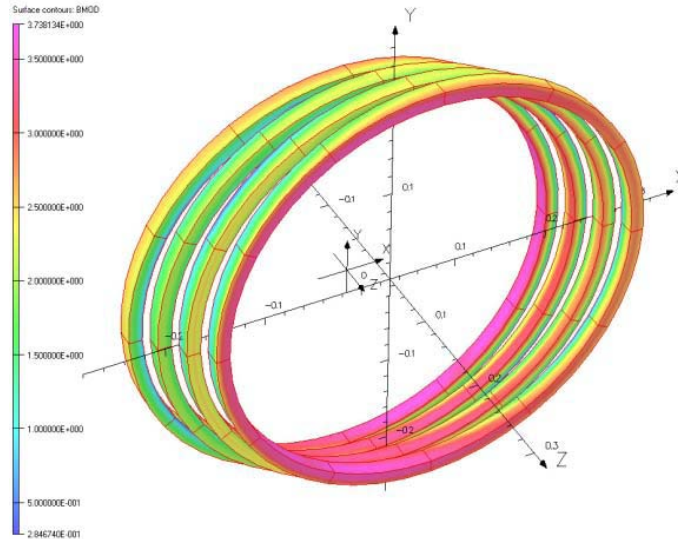


Figure 25 *Geometry of the 4-coil test model magnet, configured for VMTF dewar. The color scale shows the flux density.*

Magnets tested in a vertical dewar cryostat are typically tested using a “top hat”, which provides electrical connections and serves as the room temperature interface of the helium volume. The magnet is hung from support rods from this top hat plate. Power leads and instrumentation feedthroughs come through top hat penetrations.

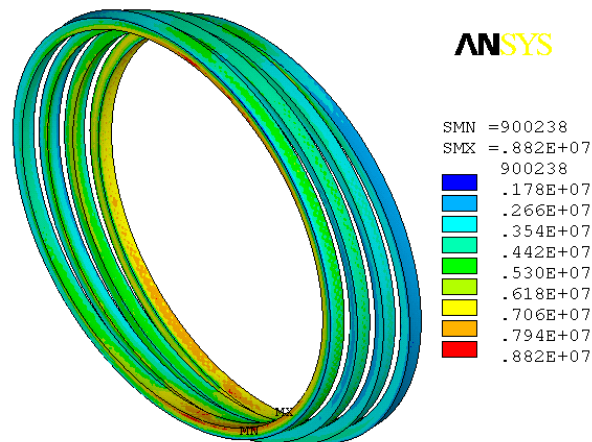


Figure 26 *Coil stress at peak current of 14 kiloAmp*

The stress analysis of the coils is shown in Figure 28.

An illustration of the 4-coil assembly is shown in Figure 29. The maximum stress in the support structure is ~23 MPa, as shown in Fig. 29, which is acceptable.

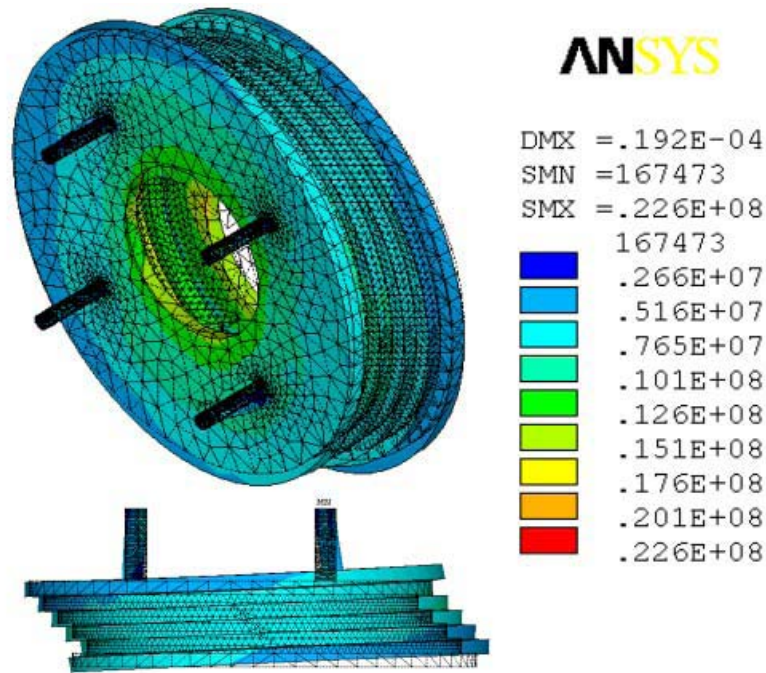


Figure 27 Model of the coils, support structure and mounting rods, with the stress and deformation analysis results indicated.

Tests will be performed in the Fermilab VMTF, The test will consist of the operation of the coils at full operational field. Magnetic measurements will be performed to determine field quality. Strain gauges will be used to determine the mechanical stress of the coils and coil support structure.

The 4-coil model is shown in Figure 30, during construction.

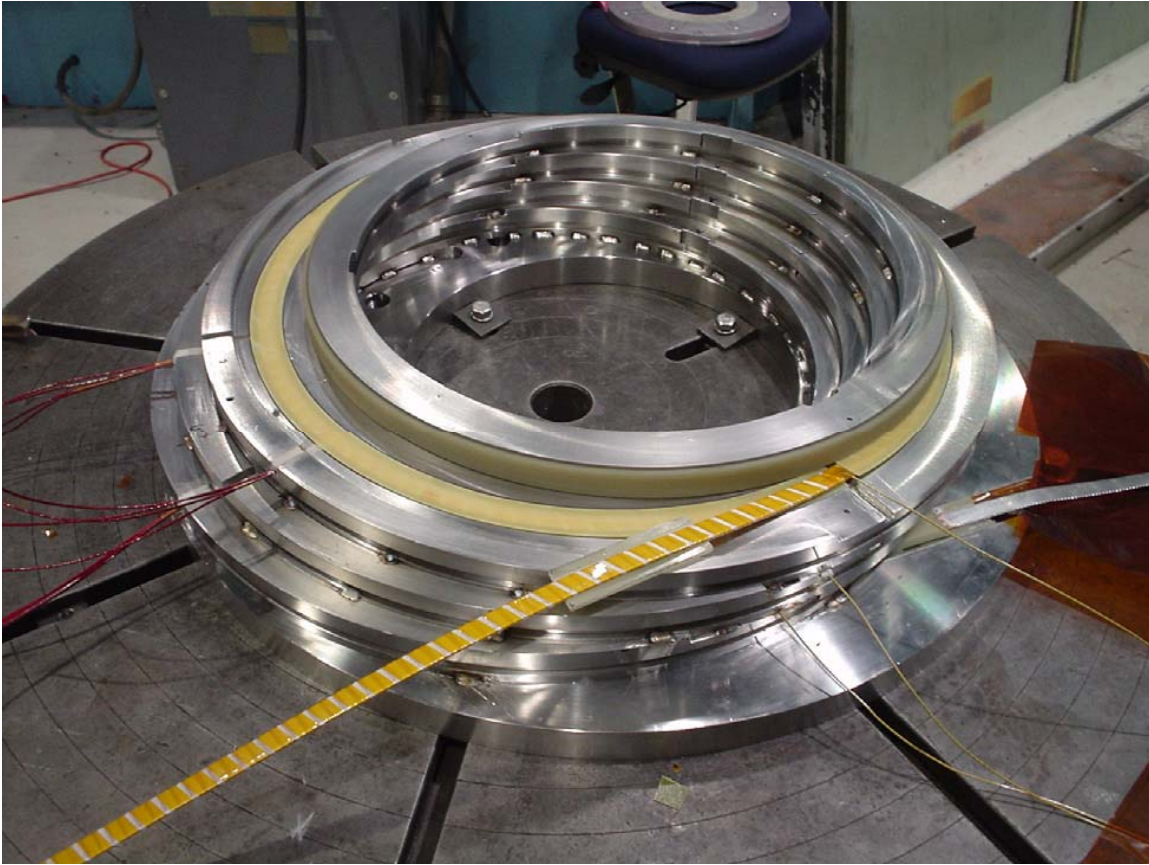


Figure 28 *Assembly of 4-coil model before 4th coil has been wound*

Status as of Dec. 5, 2008. After several quenches the magnet reached a quench limit of about 13500 amperes at 4.2K. This is quite a bit higher than the required ~9.5 kA during operation on a long string HCC, but the field is lower in this 4 coil configuration. We have not done all the analysis, the forces are different on this magnet configuration but the magnitude is comparable to the likely MANX operation. So we are quite pleased with the results. The test is very successful: good news for the Muons Inc/Fermilab collaboration!

Appendix C. Application of HCC to Produce Intense stopping Muon Beams for the Mu2e Experiment

Muons, Inc. and Fermilab have received a Phase I SBIR grant to study the use of cooling techniques to develop effective muon stopping beams. In the proposal for this grant a preliminary study indicated that a MANX-like HCC channel could increase the flux of stopping muons in the Mu2e experiment, essentially by shifting the higher flux region of the muon production spectrum downward to lower momentum. Simultaneous momentum cooling is required when the energy is degraded to compensate for the natural momentum heating that is a consequence of the unfavorable slope of the dE/dx as a function of momentum curve. A paper describing this study was reported at EPAC08 [6].

The Phase II grant will be to develop the concept described above and to study mitigation approaches to suppress backgrounds for rare event searches. In the Phase II proposal we expect to be able to push the idea of beam cooling for better stopping beams further, where more beam cooling using RF regeneration in the cooling channel can produce even brighter stopping beams. Such a cooling channel would be a natural step to the cooling channels needed for a muon collider or high-energy neutrino factory.

The scheme as described in reference 22 consists of a “dipole and wedge” following a production target, in which the combination of momentum dispersion and varying energy loss in the wedge produces an approximately monoenergetic beam of pions and muons, as indicated in Figure 31. This beam enters a HCC, in which more of the pions decay and the muons are cooled to produce a high intensity muon beam. As the end result is to be a stopped muon beam, no RF is present to restore the lost energy.

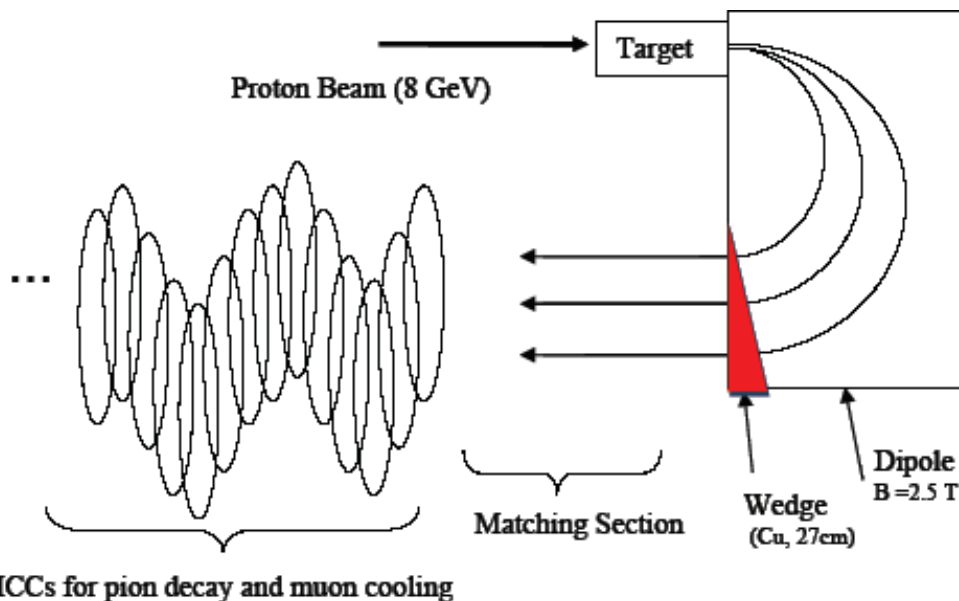


Figure 29 Scheme for use of an HCC in the production of intense muon beams

References

-
- [1] Y. Derbenev and R. P. Johnson, PHYSICAL REVIEW SPECIAL TOPICS - ACCELERATORS AND BEAMS **8**, 041002 (2005).
<http://www.muonsinc.com/reports/PRSTAB-HCCtheory.pdf>
- [2] Vladimir Kashikhin, Vadim Kashikhin, Michael Joseph Lamm, Gennady Romanov, Katsuya Yonehara, Alexander V. Zlobin, Rolland Paul Johnson, Stephen Alan Kahn, Thomas Roberts, MAGNETS FOR THE MANX 6-D MUON COOLING DEMONSTRATION EXPERIMENT.
<http://pac07.org/proceedings/PAPERS/MOPAS012.PDF>
- [3] K. Yonehara, Y. Derbenev, R. P. Johnson, T. J. Roberts, STUDIES OF A GAS-FILLED HELICAL MUON BEAM COOLING CHANNEL
<http://accelconf.web.cern.ch/AccelConf/e06/PAPERS/WEPLS016.PDF>
- [4] Derbenev and Kondratenko
- [5] J. Schwartz, NHMFL, Tallahassee, Florida R. P. Johnson, S. A. Kahn, M. Kuchnir Muons, Inc, Batavia, "Multi-purpose Fiber Optic Sensors for HTS Magnets" EPAC08, <http://accelconf.web.cern.ch/AccelConf/e08/papers/wepd023.pdf>
- [6] M. A.C. Cummings, R. J. Abrams, R. P. Johnson, C. Y. Yoshikawa C. M. Ankenbrandt, M. A. Martens, D. V. Neuffer, K. Yonehara, Intense Stopping Muon Beams, EPAC08, Genoa, Italy.
<http://accelconf.web.cern.ch/AccelConf/e08/papers/mopp071.pdf>
- [7] Muon Ionization Cooling Experiment web site, <http://mice.iit.edu/>
- [8] K. Yonehara, D. R. Broemmelsiek, M. Hu, A. Jansson, V. Kashikhin, V. S. Kashikhin, M. J. Lamm, M. L. Lopes, V. D. Shiltsev, V. Yarba, M. Yu, A. V. Zlobin, R. J. Abrams, M. A.C. Cummings, R. P. Johnson, S. A. Kahn, T. J. Roberts, "Status of the MANX Cooling Experiment", Proceedings EPAC08, Genoa, Italy, <http://accelconf.web.cern.ch/AccelConf/e08/papers/wepp153.pdf>
- [9] The SBIR (Small Business Innovation Research) and STTR (Small business Technology Transfer pRogram) are funded by the U.S. federal government.
- [10] V.S. Kashikhin, et al., "Superconducting magnetsystem for muon beam cooling", Proceedings of Applied Superconductivity Conference, ASC 2006, p. 1055.
- [11] Vladimir Kashikhin, Vadim Kashikhin, Michael Lamm, Gennady Romanov, Katsuya Yonehara, Alexander Zlobin, Rolland Johnson, Stephen Kahn, Thomas Roberts, <http://pac07.org/proceedings/PAPERS/MOPAS012.PDF>
- [12] K. Yonehara et al., PAC07, <http://pac07.org/proceedings/PAPERS/THPMN110.PDF>

-
- [13] J. Norem, et al, "Recent Results from the MuCool Test Area", Proceedings of PAC07, Albuquerque, N.M., Paper WEPMN090
- 14 M. A.C. Cummings, R. J. Abrams, R. P. Johnson, C. Y. Yoshikawa
C. M. Ankenbrandt, M. A. Martens, D. V. Neuffer, K. Yonehara
<http://accelconf.web.cern.ch/AccelConf/e08/papers/mopp071.pdf>
- [15] A. Afanasev, R. P. Johnson, Y. S. Derbenev, "Aberration-free Muon Transport Line for Extreme Ionization Cooling: a Study of Epicyclic Helical Channel" EPAC08,
<http://accelconf.web.cern.ch/AccelConf/e08/papers/wepp147.pdf>
- [16] Y. Derbenev, *Ionization Cooling on Spiral Orbit, complete linear theory*,
<http://www-mucool.fnal.gov/mcnotes/public/ps/muc0108/muc0108.ps.gz>
- [17] Y. Derbenev, COOL05.
http://www.muonsinc.com/reports/COOL05_PIC_and_REMEX_for_MC.pdf
- [18] Low Emittance Muon Collider Workshops, <http://www.muonsinc.com/mcwfeb06/>,
<http://www.muonsinc.com/mcwfeb07/>, <http://www.muonsinc.com/mcwapr08/>
- [19] Fukun Tang, "New Developments in Fast-Sampling Analog Readout of MCP-Based Large-Area Picosecond Time-of-Flight Detectors" (IEEE08, October, 2008; Dresden Germany). http://psec.uchicago.edu/Documents/tang_abs_IEEE-MIC08.pdf
- [20] Camden Ertley et al, "Development of Picosecond-Resolution Large-Area Time-of-Flight Systems", (SORMA08, June 2008; Berkeley, CA).
http://psec.uchicago.edu/Documents/SORMA08_poster.ppt
- [21] H. Frisch, "Fast Timing and TOF in HEP" (Oct 14, 2008, Lyon France).
http://hep.uchicago.edu/~frisch/talks/Lyon_Workshop_Oct15_final.ppt
- [22] Muons, Inc. and NIU submitted an SBIR proposal in November, 2008 to test SiPMs and scintillating fibers in a liquid helium environment and to develop integrated electronic readout to use with SiPMs.
- [23] B. Dolgoshein, et al, Nucl.Instr. and Meth., 563, 368 (2006).
- [24] Blondel 08
- [25] MICE Collaboration Meeting, October 19-22, 2008 at RAL,
<http://www.mice.iit.edu/cm/cm22/cm22.html>
- [26] M. Lamm, "4 Coil Magnet Status", MANX Collaboration Meeting, July 14-15, 2008
- [27] Fermilab Muon Collider Task Force Report.

http://mctf.fnal.gov/annual-reports/mctf-report-2007_v9.doc

[28] <https://mctf.fnal.gov/annual-reports/muon-5-year-documents-r5.pdf/download>

[29] V. S. Kashikhin, et al, "Four-Coil Superconducting Solenoid Model for Muon Beam Cooling", Proceedings of EPAC08, Genoa, Italy, Paper WEPD013